Simulating *Ips typographus (L.)*, outbreak dynamics and their influence on carbon balance estimates with ORCHIDEE r8627

Guillaume Marie[1]*, Jina Jeong[2]*, Hervé Jactel[3], Gunnar Petter[4], Maxime Cailleret[5], Matthew J. McGrath[1], Vladislav Bastrikov[6], Josefine Ghattas[7], Bertrand Guenet[8], Anne Sofie Lansø[9], Kim Naudts[11], Aude Valade[10], Chao Yue[12], Sebastiaan Luyssaert[2]

[1] Laboratoire des Sciences du Climat et de l'Environnement, CEA CNRS UVSQ UP Saclay, 91191 Orme des Merisiers, Gif-sur-Yvette, France

[2] Faculty of Science, A-LIFE, Vrije Universiteit Amsterdam, 1081 BT Amsterdam, the Netherlands

[3] INRAE, University of Bordeaux, UMR Biogeco, 33612 Cestas, France

[4] ETH Zürich, Department of Environmental Systems Science, Forest Ecology, 8092 Zürich, Switzerland

[5] INRAE, Aix-Marseille Univ, UMR RECOVER, 13182 Aix-en-Provence, France

[6] Science Partner, France

[7] Institut Pierre-Simon Laplace – Sciences du climat (IPSL), 75105 Jussieu, France

[8] Laboratoire de Géologie, Ecole Normale Supérieure, CNRS, PSL Research University, IPSL, 75005 Paris, France

[9] Department of Environmental Science, Aarhus Universitet, Frederiksborgvej 399, 4000 Roskilde, Denmark

[10] Eco & Sols, Univ Montpellier, CIRAD, INRAE, 34060 Institut Agro, IRD, Montpellier, France

[11] Department of Earth Sciences, Vrije Universiteit Amsterdam, 1081 HV Amsterdam, the Netherlands

[12] State Key Laboratory of Soil Erosion and Dryland Farming on the Loess Plateau, Northwest A & F University, Yangling, Shaanxi, China

* These authors contributed equally to this study

Corresponding author: Guillaume Marie, guillaume.marie@lsce.ipsl.fr, Jina Jeong, j.jeong@vu.nl, Sebastiaan Luyssaert, s.luyssaert@vu.nl

Abstract : New (a)biotic conditions resulting from climate change are expected to change disturbance dynamics, such as windthrow, forest fires, droughts, and insect outbreaks, and their interactions. These unprecedented natural disturbance dynamics might alter the capability of forest ecosystems to buffer atmospheric CO_2 increases, potentially leading forests to transform from sinks into sources of CO_2. This study aims to enhance the ORCHIDEE land surface model to study the impacts of climate change on the dynamics of the bark beetle *Ips typographus* and subsequent effects on forest functioning. The *Ips typographus* outbreak model is inspired by previous work from Temperli et al. 2013 for the LandClim landscape model. The new implementation of this model in ORCHIDEE r8627 accounts for key differences between ORCHIDEE and LandClim: (1) the coarser spatial resolution of ORCHIDEE, (2) the higher

temporal resolution of ORCHIDEE, and (3) the pre-existing process representation of windthrow, drought, and forest structure in ORCHIDEE. Simulation experiments demonstrated the capability of ORCHIDEE to simulate a variety of post-disturbance forest dynamics observed in empirical studies. Through an array of simulation experiments across various climatic conditions and windthrow intensities, the model was tested for its sensitivity to climate, initial disturbance, and selected parameter values. The results of these tests indicated that with a single set of parameters, ORCHIDEE outputs spanned the range of observed dynamics. Additional tests highlighted the substantial impact of incorporating *Ips typographus* outbreaks on carbon dynamics. Notably, the study revealed that modeling abrupt mortality events, as opposed to a continuous mortality framework, provides new insights into the short-term carbon sequestration potential of forests under disturbance regimes by showing that the continuous mortality framework tends to overestimate the carbon sink capacity of forests in the 20 to 50 year range in ecosystems under high disturbance pressure, compared to scenarios with abrupt mortality events. This model enhancement underscores the critical need to include disturbance dynamics in land surface models to refine predictions of forest carbon dynamics in a changing climate.

1. Introduction

Future climate will likely bring new abiotic constraints through the co-occurrence of multiple connected hazards, e.g., "hotter droughts", which are droughts combined with heat waves (Allen et al., 2015; Zscheischler et al., 2018), but also new biotic conditions from interacting natural and anthropogenic disturbances, e.g., insect outbreaks following windthrow or forest fires (Seidl et al., 2017). Unprecedented natural disturbance dynamics might alter biogeochemical cycles specifically the capability of forest ecosystems to buffer the CO_2 increase in the atmosphere (Hicke et al., 2012; Seidl et al., 2014) and the risk that forests are transformed from sinks into sources of CO_2 (Kurz et al., 2008a). The magnitude of such alteration, however, remains uncertain principally due to the lack of impact studies that include disturbance regime shifts at global scale (Seidl et al., 2011).

Land surface models are used to study the relationships between climate change and the biogeochemical cycles of carbon, water, and nitrogen (Ciais et al., 2005; Cox et al., 2000; Friedlingstein et al., 2006; Luyssaert et al., 2018; Zaehle and Dalmonech, 2011). Many of these models use background mortality to obtain an equilibrium in their biomass pools. This classic approach towards forest dynamics, which assumes steady-state conditions over long periods of time, may not be suitable for assessing the impacts of disturbances on shorter time scales under a fast changing climate. This could be considered a shortcoming in the land surface models because disturbances can have significant impacts on ecosystem services, such as water regulation, carbon sequestration, and biodiversity (Quillet et al., 2010). Mechanistic approaches that account for a variety of mortality causes, such as age, size, competition, climate, and disturbances, are now being considered and tested to simulate forest dynamics more accurately (Migliavacca et al., 2021). For example, the land surface model ORCHIDEE accounts for mortality from interspecific competition for light in addition to background mortality (Naudts et al., 2015). Implementing a more mechanistic view on mortality is thought to be essential for improving our understanding of the impacts of climate change on forest dynamics and the provision of ecosystem services.

73

74 Land surface models also face the challenge of better describing mortality particularly when it comes to ecosystem
75 responses to "cascading disturbances", where legacy effects from one disturbance affect the next (Buma, 2015;
76 Zscheischler et al., 2018). Biotic disturbances, such as bark beetle outbreaks, strongly depend on previous
77 disturbances as their infestation capabilities are higher when tree vitality is low, for example following drought or
78 storm events (Seidl et al., 2018). This illustrates how interactions between biotic and abiotic disturbances can have
79 substantial effects on ecosystem dynamics and must be accounted for in land surface models to improve our
80 understanding of the impacts of climate change on forest dynamics (Seidl et al., 2011; Temperli et al., 2013a). While
81 progress has been made towards including abrupt mortality from individual disturbance types such as wildfire
82 (Lasslop et al., 2014; Migliavacca et al., 2013; Yue et al., 2014), windthrow (Chen et al., 2018) and drought (Yao et
83 al., 2022), the interaction of biotic and abiotic disturbances remains both a knowledge and modeling gap (Kautz et
84 al., 2018).

85

86 Bark beetle infestations are increasingly recognized as disturbance events of regional to global importance (Bentz et
87 al., 2010; Kurz et al., 2008b; Seidl et al., 2018). Notably, a bark beetle outbreak ravaged over 90% of Engelmann
88 spruce trees across approximately 325,000 hectares in the Canadian and American Rocky Mountains between 2005
89 and 2017 (Andrus et al., 2020). In Europe, the bark beetle *Ips typographus* has been involved in up to 8% of total
90 tree mortality due to natural disturbances from 1850 to 2000 (Hlásny et al., 2021a). A recent increase in beetle
91 activity, particularly following mild winters (Andrus et al., 2020; Kurz et al., 2008c), windthrow (Mezei et al.,
92 2017), and droughts (Nardi et al., 2023) have been well-documented (Hlásny et al., 2021a; Pasztor et al., 2014),
93 underscoring the need to integrate bark beetle dynamics into land surface modeling.

94

95 Past studies used a variety of approaches to model the impacts of bark beetles on forests. While some models treated
96 bark beetle outbreaks as background mortality (Luyssaert et al., 2018; Naudts et al., 2016), others dynamically
97 modeled these outbreaks within ecosystems (Jönsson et al., 2012; Seidl and Rammer, 2016; Temperli et al., 2013b).
98 Studies with prescribed beetle outbreaks tend to focus on the direct effects of the outbreak on forest conditions and
99 carbon fluxes, but are likely to overlook more complex feedback processes, such as interactions with other
100 disturbances and longer-term impacts. Conversely, dynamic modeling of beetle outbreaks, provides a more
101 comprehensive view by incorporating the lifecycle of bark beetles, tree defense mechanisms, and ensuing alterations
102 in forest composition and functionality.

103

104 Simulation experiments for *Ips typographus* outbreaks using the LPJ-GUESS vegetation model highlighted regional
105 variations in outbreak frequencies, pinpointing climate change as a key exacerbating factor (Jönsson et al., 2012).
106 Simulation experiments with the iLand landscape model suggested that almost 65% of *Ips typographus* outbreaks are
107 aggravated by other environmental drivers (Seidl and Rammer, 2016). A 4°C temperature increase could result in a
108 265% increase in disturbed area and a 1800% growth in the average patch size of the disturbance (Siedl and Rammer
109 2016). Disturbance interactions were ten times more sensitive to temperature changes, boosting the disturbance

110 regime's climate sensitivity. The results of these studies justify the inclusion of interacting disturbances in land
111 surface models, such as ORCHIDEE, which are used in future climate predictions and impact studies (Boucher et al.,
112 2020).
113
114 The objectives of this study are: (1) to develop and implement a spatially implicit outbreak model for *Ips*
115 *typographus* in the land surface model ORCHIDEE inspired by the work from Temperli et al. (2013), and (2) use
116 simulation experiments to characterize the behavior of this newly added model functionality.
117

2. Model description

2.1. The land surface model ORCHIDEE

120 ORCHIDEE is the land surface model of the IPSL (Institut Pierre Simon Laplace) Earth system model (Boucher et
121 al., 2020; Krinner et al., 2005). ORCHIDEE can, however, also be run uncoupled as a stand-alone land surface
122 model forced by temperature, humidity, pressure, precipitation, and wind fields. Unlike the coupled setup, which
123 needs to run on the global scale, the stand-alone configuration can cover any area ranging from a single grid point to
124 the global domain. In this study ORCHIDEE was run as a stand-alone land surface model.
125
126 ORCHIDEE does not enforce any particular spatial resolution. The spatial resolution is an implicit user setting that
127 is determined by the resolution of the climate forcing (or the resolution of the atmospheric model in a coupled
128 configuration). ORCHIDEE can run on any temporal resolution. This apparent flexibility is somewhat restricted as
129 processes are formalized at given time steps: half-hourly (e.g., photosynthesis and energy budget), daily (i.e., net
130 primary production), and annual (i.e. vegetation demographic processes). With the current model architecture
131 meaningful simulations should have a temporal resolution of one minute to one hour for the calculation of energy
132 balance, water balance, and photosynthesis.
133
134 ORCHIDEE utilizes meta-classes to discretize the global diversity in vegetation. The model includes 13 meta-
135 classes by default, including one class for bare soil, eight classes for various combinations of leaf-type and climate
136 zones of forests, two classes for grasslands, and two classes for croplands. Each meta-class can be further subdivided
137 into an unlimited number of plant functional types (PFTs). The current default setting of ORCHIDEE distinguishes
138 15 PFTs where the meta-class of C3 grasslands have been separated into a boreal, temperate and tropical C3
139 grassland PFT.
140
141 At the beginning of a simulation, each forest PFT in ORCHIDEE contains a monospecific forest stand that is
142 structured by a user-defined but fixed number of diameter classes (three by default). Throughout the simulation, the
143 boundaries of the diameter classes are adjusted to accommodate changes in the stand structure, while the number of
144 classes remains constant. Flexible class boundaries provide a computationally efficient approach to simulate
145 different forest structures. For instance, an even-aged forest is simulated by using a small diameter range between
146 the smallest and largest trees, resulting in all trees belonging to the same stratum. Conversely, an uneven-aged forest

147 is simulated by applying a wide range between diameter classes, such that different classes represent different
148 canopy strata.
149
150 The model uses allometric relationships to link tree height and crown diameter to stem diameter. Individual tree
151 canopies are not explicitly represented, instead a canopy structure model based on simple geometric forms (Haverd
152 et al. 2012) has been included in ORCHIDEE (Naudts et al., 2015). Diameter classes represent trees with different
153 mean diameter and height, which informs the user about the social position of trees within the canopy. Intra-stand
154 competition is based on the basal area of individual trees, which accounts for the fact that trees with a higher basal
155 area occupy dominant positions in the canopy and are therefore more likely to intercept light and thus contribute
156 more to stand-level photosynthesis and biomass growth compared to suppressed trees (Deleuze et al., 2004). If
157 recruitment occurs, diameter classes evolve into cohorts. However, in the absence of recruitment, all diameter
158 classes contain trees of the same age.
159
160 Individual tree mortality from self-thinning, wind storms, and forest management is explicitly simulated. Other
161 sources of mortality are implicitly accounted for through a so-called constant background mortality rate.
162 Furthermore, age classes (four by default) can be used after land cover change, forest management, and disturbance
163 events to explicitly simulate the regrowth of the forest. Following a land cover change, biomass and soil carbon
164 pools (but not soil water columns) are either merged or split to represent the various outcomes of a land cover
165 change. The ability of ORCHIDEE to simulate dynamic canopy structures (Chen et al., 2016; Naudts et al., 2015b;
166 Ryder et al., 2016), a feature essential to simulate both the biogeochemical and biophysical effects of natural and
167 anthropogenic disturbances, is exploited in other parts of the model, i.e., precipitation interception, transpiration,
168 energy budget calculations, the radiation scheme, and the calculation of the absorbed light for photosynthesis.
169
170 Since revision 7791, mortality from *Ips typographus* outbreaks is explicitly accounted for and thus conceptually
171 excluded from the so-called environmental background mortality. Subsequently, changes in canopy structure
172 resulting from growth, forest management, land cover changes, wind storms, and *Ips typographus* outbreaks are
173 accounted for in the calculations of the carbon, water, and energy exchanges between the land surface and the
174 atmosphere. For details on the functionality of the ORCHIDEE model that is not of direct relevance for this study,
175 e.g., energy budget calculations, soil hydrology, snow phenology, albedo, roughness, photosynthesis, respiration,
176 phenology, carbon and nitrogen allocation, land cover changes, product use, and the nitrogen cycle are readers are
177 referred to Krinner et al., 2005; Zaehle and Friend, 2010; Naudts et al., 2015; Vuichard et al., 2019.
178
179   **2.2.**   **Origin of the bark beetle (*Ips typographus*) model: the LANDCLIM legacy**
180 Although mortality from windthrow (Yi-Ying et al., 2018) and forest management (Luyssaert et al., 2018; Naudts et
181 al., 2016) were already accounted for in ORCHIDEE prior to r8627, insect outbreaks and their interaction with other
182 disturbances were not. The LandClim model (Schumacher, 2004) and more specifically the *Ips typographus* model
183 developed by Temperli et al. (2013) has been used as basis to develop the *Ips typographus* model in ORCHIDEE

184 r8627.

185

186 LandClim is a spatially explicit stochastic landscape model in which forest dynamics are simulated at a yearly time
187 step for 10–100 km² landscapes consisting of 25 m × 25 m patches. Within a patch recruitment, growth, mortality
188 and competition among age cohorts of different tree species are simulated with a gap model (Bugmann, 1996) in
189 response to monthly mean temperature, climatic drought, and light availability. LandClim, for which a detailed
190 description can be found in (Schumacher, 2004; Temperli et al., 2013), includes the functionality to simulate the
191 decadal dynamics and consequences of *Ips typographus* outbreaks at the landscape-scale (Temperli et al., 2013). In
192 the LandClim approach, the extent, occurrence and severity of beetle-induced tree mortality are driven by the
193 landscape susceptibility, beetle pressure, and infested tree biomass. While the LandClim beetle model was designed
194 and structured to be generally applicable for northern hemisphere climate-sensitive bark beetle-host systems, it was
195 parameterized to represent disturbances by the *Ips typographus* in Norway spruce (*Picea abies* Karst.; Temperli et
196 al. 2013).

197

198 As LandClim and ORCHIDEE are developed for different purposes, their temporal and spatial scales differ. These
199 differences in model resolution justify developing a new model while following the principles embedded in the
200 LandClim approach. LandClim assesses bark beetle damage at 25 m x 25 m patches and to do so it uses information
201 from other nearby patches as well as landscape characteristics such as slope, aspect and altitude. The susceptibility
202 of a landscape to bark beetle infestations is calculated using multiple factors such as drought-induced tree resistance,
203 age of the oldest spruce cohort, proportion of spruce in the patch's basal area, and spruce biomass damaged by
204 windthrow. These drivers are presented as sigmoidal relationships ranging from 0 to 1 (denoting none to maximum
205 susceptibility respectively) that are combined in a susceptibility index for each Norway spruce cohort in a patch.
206 Bark beetle pressure is quantified as the potential number of beetles that can infest a patch, and its calculation
207 considers, among others, previous beetle activity, maximum possible spruce biomass that beetles could kill, and
208 temperature-dependent bark beetle phenology. Finally, the susceptibility index and beetle pressure are used to
209 estimate the total infested tree biomass and total biomass killed by bark beetles for each cohort within a patch.

210

211 In ORCHIDEE, however, the simulation unit is about six orders of magnitude larger, i.e. 25 km x 25 km. Hence, a
212 single gridcell in ORCHIDEE exceeds the size of an entire landscape in LandClim. Where landscape characteristics
213 in LandClim can be represented by statistical distributions, the same characteristics in ORCHIDEE are represented
214 by single values. These differences between LandClim and ORCHIDEE imply that the original bark beetle model
215 cannot be implemented in ORCHIDEE without substantial adjustments; the model at the ORCHIDEE gridcell
216 should work without requiring spatial information and statistical distributions of landscape characteristics because
217 those are not available in ORCHIDEE.

218

219

220

221 **2.3. Bark beetle outbreak development stages**

222 Bark beetle outbreak development stages (Fig. 1) are useful to understand the dynamics of an outbreak (Edburg et

223 al., 2012; Hlásny et al., 2021a; Wermelinger, 2004). Nonetheless, the outbreak model in ORCHIDEE r8627

224 simulates the dynamic of the Ips *typographus* outbreak as a continuous process. Hence, endemic, epidemic, build-up

225 and post-epidemic stages are not explicitly simulated. In this study, outbreak development stages were only

226 introduced to structure the model description. If needed, these stages could be distinguished while post-processing

227 the simulation results if (arbitrary) thresholds are set for specific variables such as $DR_{beetles}$.
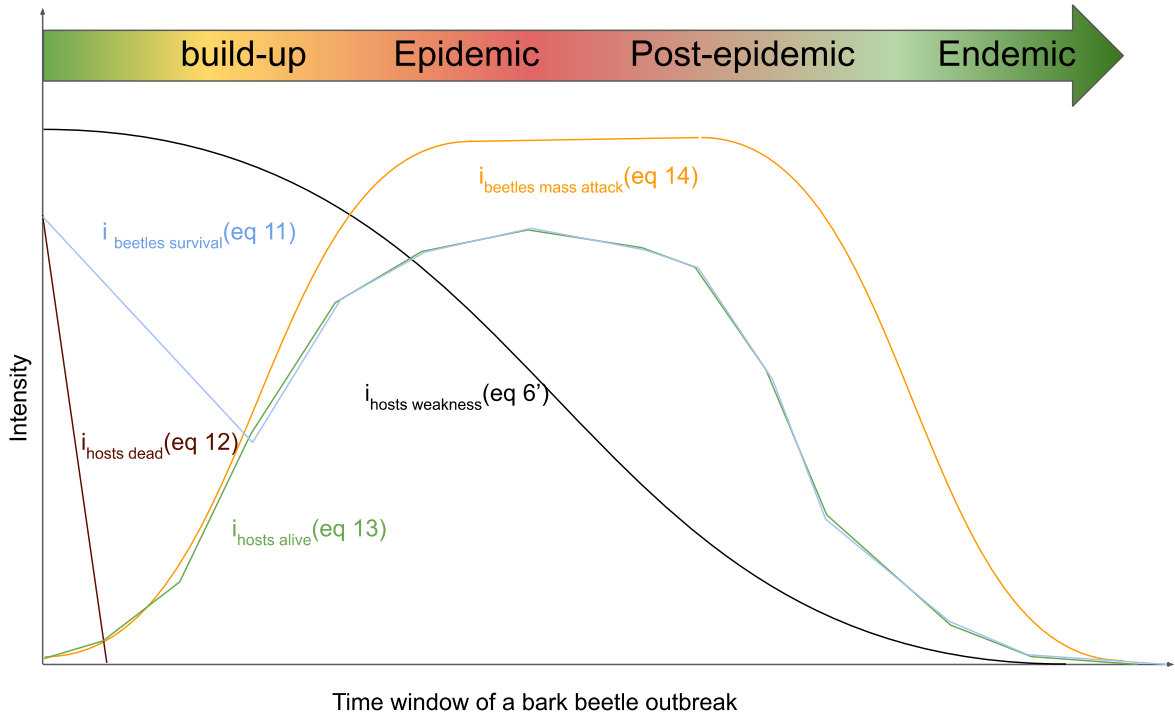

Time window of a bark beetle outbreak

Figure 1 : Dynamic interplay of the different host and beetle characteristics during a bark beetle (*Ips typographus*) outbreak. The time window spans four outbreak development stages: build-up, epidemic, post-epidemic, and endemic. The curves represent key characteristics, showing the growth in beetle population and subsequent decline in host population. $I_{hosts\ dead}$ characterizes the presence of defenseless uprooted or cut spruce trees; $i_{hosts\ alive}$, characterizes living spruce trees that could become hosts for the bark beetles; $i_{hosts\ susceptibility}$, susceptibility of spruce trees to bark beetle attack; $i_{beetles\ mass\ attack}$, quantifies the capability of the bark beetles to mass attack; $i_{beetles\ survival}$, characterizes the survival of bark beetles. Host and bark beetle characteristics are detailed in the subsequent text. When the density of the host trees is declining due to an increased host mortality from the bark beetle outbreak itself, the competition between trees for light and nutrients declines as well. As a consequence, the host susceptibility decreases which in ORCHIDEE is the main pathway for an outbreak to move back to the endemic phase. After 1 year the wood from a storm is not fresh enough for bark beetles to breed in. In ORCHIDEE, the bark beetle population needs to be capable of mass attacking living trees within a year to make the transition from the build-up to the epidemic phase.

228

229   **2.4.   bark beetle (*Ips typographus*) damage in ORCHIDEE**

Table 1: List of symbols

Symbol	Description	Units
α	Intercept of the self thinning relationship	unitless
β	Exponent of the self thinning relationship	unitless
act_{limit}	B_{kill}/B_{total} at which $i_{beetles\ activity} = 0.5$	$gC.m^{-2}$
$B_{beetles\ kill}$	Biomass of spruce killed by bark beetle annually	$gC.m^{-2}$
$B_{windthrow\ kill}$	Biomass of spruce killed by windthrow event	$gC.m^{-2}$
$B_{beetles\ attacked}$	Biomass of spruce attacked by bark beetle annually	$gC.m^{-2}$
B_{total}	Total living biomass of spruce stand	$gC.m^{-2}$
B_{wood}	Woody biomass of spruce stand	$gC.m^{-2}$
BP_{limit}	$i_{beetle\ pressure}$ at which $i_{beetles\ mass\ attack} = 0.5$	unitless
D_{max}	Maximum stand density	$tree.ha^{-1}$
$D_{age\ class}$	Stand tree density of spruce age classes	$tree.ha^{-1}$
D_{spruce}	Stand tree density of spruce	$tree.ha^{-1}$
DD_{eff}	Cumulative effective degrees days	$°C.Day^{-1}$
DD_{ref}	Reference degrees days to complete one beetle generation	$°C.Day^{-1}$
$Dia_{quadratic}$	Mean quadratic diameter	meters
$DR_{beetles}$	$B_{beetles\ kill}/B_{total} * 100$	%
$DR_{windthrow}$	$B_{windtrow\ kill}/B_{total} * 100$	%
F_{spruce}	Area fraction of spruce within gridcell	unitless
$F_{age\ class}$	Area fraction of spruce age classes	unitless
$F_{non-spruce}$	Non-spruce area fraction	unitless
G_{limit}	Beetles generation number at which $i_{beetle\ generation} = 0.5$	Generation
$I_{hosts\ competition}$	Spruce trees under competition pressure	unitless
$I_{hosts\ susceptibility}$	Spruce trees susceptibility to bark beetle attack	unitless
$I_{hosts\ attractivity}$	Spruce attractivity for bark beetles	unitless
$I_{hosts\ dead}$	Defenseless spruce trees uprooted or cut	unitless
$I_{hosts\ alive}$	Potential living hosts for bark beetle	unitless
$I_{hosts\ defense}$	Spruce trees capability to resist a bark beetle attack	unitless
$I_{hosts\ share}$	Spruces hidden by other species to bark beetle detection	unitless
$I_{hosts\ competition,\ age\ class}$	Spruce age class under competition pressure	unitless
$I_{hosts\ defense,\ age\ class}$	Spruce age class capability to resist a bark beetle attack	unitless
$I_{hosts\ health,\ age\_class}$	Spruce age class health condition	unitless
$I_{beetles\ pressure}$	Proxy of bark beetle population level	unitless
$I_{beetles\ survival}$	Bark beetle survival index	unitless
$I_{beetles\ generation}$	Bark beetle generation index	unitless
$i_{beetles\_activity}$	Previous bark beetles activity index	unitless
$i_{beetles\_mass\_attack}$	Bark beetles mass attack capability	unitless
max_{Nwood}	Value of N_{wood} at which $i_{hosts\ dead} = 1.0$	unitless
N_{wood}	Spruce woody necromass	$gC.m^{-2}$
$P_{success,\ age\_class}$	Probability of successful attack per age class	unitless
P_{attack}	Probability of beetles attack	unitless
PWS_{max}	Maximum long term spruce water stress	unitless
PWS_{spruce}	Spruce water stress	unitless
PWS_{age_class}	Spruce age classes water stress	unitless
PWS_{limit}	Spruce water stress at which $i_{hosts\ defense} = 0.5$	unitless
i_{rd_limit}	Relative density index at which $i_{hosts\ competition} = 0.5$	unitless
$i_{rd\_susceptibility}$	Relative density index at which $i_{host\ susceptibility} = 0.5$	unitless
i_{rd_spruce}	Spruce stand relative density index [0,1]	unitless
$I_{rd,\ age\ class}$	Spruce age classes relative density index [0,1]	unitless
$S_{competition}$	Shape parameter in the calculation of $i_{hosts\ competition}$	unitless
$S_{susceptibility}$	Shape parameter in the calculation of $i_{hosts\ susceptibility}$	unitless

$S_{drought}$	Shape parameter in the calculation of $i_{hosts\ defense}$	unitless
S_{share}	Shape parameter in the calculation of $i_{hosts\ share}$	unitless
$S_{activity}$	Shape parameter in the calculation of $i_{beetle\ activity,\ y-1}$	unitless
$S_{generation}$	Shape parameter in the calculation of $i_{beetle\ generation}$	unitless
Sh_{spruce}	Share fraction of spruce against non-spruce in gridcell	unitless
Sh_{limit}	Share fraction at which $i_{hosts\ share} = 0.5$	unitless
T_{air}	Air temperature	°C
T_{max}	Temperature above which beetles developpement stop	°C
T_{min}	Temperature below which beetles developpement stop	°C
T_{bark}	Bark temperature	°C
T_{opt}	Optimal bark temperature for beetles development	°C

230

231 The biomass of trees killed by bark beetles in one year and one gridcell ($B_{beetles\ kill}$) is calculated as the product of the

232 biomass of trees attacked by bark beetles ($B_{beetles\ attacked}$) and the probability of a successful attack ($P_{success,\ age\ class}$)

233 averaged over the number of spruce age classes and weighted by their actual fraction ($F_{age\ class}$ / F_{spruce}). The approach

234 assumes that a successful beetle colonization always results in the death of the attacked tree which is a simplification

235 from reality (A. Leufvén et al. 1986).

236

237 $$B_{beetles\ kill} = \sum_{nb\ age\ classes}^{age\ class=1} P_{success,\ age\ class} \times B_{beetles\ attacked} \times \frac{F_{age\ class}}{F_{spruce}} \qquad (1)$$

238

239 During the endemic stage, $B_{beetles\ attacked}$ and $B_{beetles\ kill}$ are at their lowest values and the damage from bark beetles has

240 little impact on the structure and function of the forest. Losses from $B_{beetles\ kill}$ can be considered to contribute to the

241 background mortality.

242

243 The biomass of trees attacked by bark beetles ($B_{beetles\ attacked}$) is the outcome of bark beetles that successfully overcame

244 the tree defenses and succeeded in boring holes in the bark in order to reach the sapwood. $B_{beetles\ attacked}$ is calculated at

245 the gridcell by multiplying the actual stand biomass of spruce (B_{total}) and the probability that bark beetles attack

246 spruce trees in the gridcell ($P_{attacked}$).

247

248 $$B_{beetles\ attacked} = B_{total} \times P_{attacked} \qquad (2)$$

249

250 $P_{attacked}$ represent the ability of the bark beetles to spread and to locate new suitable spruce trees as hosts for breeding.

251 $P_{attacked}$ is calculated by the product of two indexes (all indexes in this study are denoted i and are analogue the

252 susceptibility indexes from Temperli et al. 2013): (1) the beetle pressure index ($i_{beetles\ pressure}$) which a proxy of the bark

253 beetle population and (2) the stand attractivity index ($i_{hosts\ attractivity}$) is related to its health and reflects the ability of the

254 forest to resist an external stressor such as bark beetle attacks.

255

256 $$P_{attacked} = i_{hosts\ attractivity} \times i_{beetles\ pressure} \qquad (3)$$

257

2.5.   Host attractivity

The stand attractivity index ($i_{hosts\ attractivity}$) represents how interesting a stand is for a new bark beetle colony. When $i_{hosts\ attractivity}$ tends to 0, the stand is constituted mainly by healthy trees which are less attractive for beetles whereas an $i_{hosts\ attractivity}$ approaching 1 represents a highly stressed spruce stand suitable for colonization by bark beetles. Factors that contribute to the stress of a forest are: nitrogen limitation, limited carbohydrate reserves, and monospecific spruce forest. Trees experiencing extended periods of environmental stress are expected to have less carbon and nitrogen reserves available for defense compounds, making them vulnerable for bark beetle attacks even at relatively low beetle population densities (Raffa et al., 2008). Nonetheless, reserves pools in ORCHIDEE r8627 have not yet been evaluated so, instead proxies were used such as long term drought (PWS_{max}) and relative density index (i_{rd}) which were already simulated in ORCHIDEE r8627.

$$i_{hosts\ attractivity} = max\left(i_{hosts\ competition}, i_{hosts\ defense}\right) \times i_{hosts\ share} \qquad (4)$$

Where $i_{hosts\ competition}$ and $i_{hosts\ defense}$ both represent proxies for the reduction of the nitrogen and carbohydrate reserve due to strong competition for light and soil resources, and consecutive years that are drier than average. For this study, the max drought intensity during the last three years (PWS_{max}) is considered, as a proxy of spruce stand healthiness:

$$i_{hosts\ defense} = 1 / \left(1 + e^{S_{drought} \cdot (1 - PW S_{max} - PW S_{limit})}\right) \qquad (5a)$$

$$PW S_{max} = \sum_{nb\ age\ class=3}^{age\ class=1} max\left(PW S_{spruce,n}, PW S_{spruce,n-1}, PW S_{spruce,n-2}\right) \times \frac{F_{spruce\ class}}{F_{spruce}} \qquad (5b)$$

Where PWS_{spruce} is the average daily plant water stress index over the growing season for the spruce stand and is equal to 0 when plants are highly stressed. PWS_{limit} is the plant water stress below which the healthiness of the stand will strongly be affected. *Nb age class* is the numbers age class within the stand and is equal to 3 in this study. In addition to drought, overstocked forest may also decrease the overall healthiness of a spruce stand ($i_{hosts\ competition}$).

$$i_{hosts\ competition} = 1 / \left(1 + e^{S_{competition} \cdot (i_{rd\ spruce} - i_{rd\ limit})}\right) \qquad (6a)$$

In ORCHIDEE, the relative density index (i_{rd}) is used to quantify the competition between trees at the stand level. At an i_{rd} of 1, the forest is expected to be at its maximum density given the carrying capacity of the site, implying the highest level of competition between trees. $i_{rd\ limit}$ represents the limit at which the bark beetle outbreak starts to decline because of lack of suitable host trees. The severity of bark beetle-caused tree mortality decreases when we increase the spatial resolution from the stand to the landscape scale. At the landscape scale, which can cover areas up to 2500 km², the duration of mortality may be longer and the severity lower because beetles disperse across the landscape and cause mortality at different times. This distinction is important for interpreting model results,

293 particularly when considering parameters like $i_{rd\,limit}$ in the ORCHIDEE model. $i_{rd\,limit}$ describes the proportion of trees
294 surviving after an outbreak and should therefore be adjusted for the spatial scale of a gridcell in ORCHIDEE. In
295 model set-up where a gridcell represents a single stand (~1 ha), $i_{rd\,limit}$ should be close to 0, indicating that nearly all
296 trees may be killed. However, in a simulation with gridcells representing 2500 km², not all trees will be killed, which
297 is reflected in setting $i_{rd\,limit}$ to 0.4.

298

299 $i_{rd\,spruce}$ is computed as follows:

300

301 $$i_{rd\,spruce} = \sum_{nb\,age\,class=3}^{age\,class=1} \frac{D_{age\,class}}{D_{max}} \times \frac{F_{age\,class}}{F_{spruce}} \qquad (6b)$$

302

303 Where $D_{age\,class}$ is the current tree density of an age class and $F_{age\,class}$ is the fraction of spruce in the gridcell that
304 resides in this age class. D_{max} represents the maximum stand density of a stand given its diameter. In ORCHIDEE
305 D_{max} is calculated based on the quadratic mean diameter (cm) of the age class and two species specific parameters, α
306 and β:

307

308 $$D_{max} = \left(Dia_{quadratic,age\,class} / \alpha \right)^{(1/\beta)} \qquad (6c)$$

309

310 The index $i_{hosts\,share}$ (used in eq. 4) takes into account that in a mixed tree species landscape, even a few non-host trees
311 may chemically hinder bark beetles in finding their host trees (Zhang and Schlyter, 2004) explaining why insect
312 pests, including *Ips typographus* outbreaks, often cause more damage in pure compared to mixed stands (Nardi et al.,
313 2023). ORCHIDEE r8627 does not simulate multi-species stands but does account for landscape-level heterogeneity
314 of forests with different plant functional types. The bark beetle model in ORCHIDEE assumes that within a gridcell,
315 the fraction of spruce over other tree species is a proxy for the degree of mixture:

316

317 $$i_{hosts\,share} = 1 / \left(1 + e^{S_{share} \cdot (SH_{spruce} - SH_{limit})} \right) \qquad (7a)$$

318

319 Where,

320

321 $$Sh_{spruce} = F_{non-spruce} / F_{spruce} \qquad (7b)$$

322

2.6. Implicit representation of bark beetle populations

324 The bark beetle pressure Index $(i_{beetles\,pressure})$ is now formulated based on two components: (1) the bark beetle
325 breeding index of the current year $(i_{beetles\,generation})$, and (2) an index of the loss of tree biomass in the previous year due
326 to bark beetle infestation $(i_{beetles\,activity})$. $i_{beetles\,activity}$ is thus a proxy of the previous year's bark beetle activity. The
327 expression accounts for the legacy effect of bark beetle activities by averaging activities over the current and

329 previous years. In this approach, the susceptibility index ($i_{beetles\,survival}$) serves as an indicator for increased bark beetle

330 survival which could result from favorable conditions for beetle demography (see next section).

331

332 $$i_{beetles\,pressure} = i_{beetles\,survival} \times \frac{\left(i_{beetles\,generation} + i_{beetles\,activity} \right)}{2} \qquad (8)$$

333

334 The model calculates $i_{beetles\,generation}$ from a logistic function, which depends on the number of generations a bark beetle

335 population can sustain within a single year:

336

337 $$i_{beetles\,generation} = 1/\left(1 + e^{-S_{generation} \cdot \left(\frac{DD_{eff}}{DD_{ref}} - G_{limit} \right)} \right) \qquad (9)$$

338

339 Where $S_{generation}$ and G_{limit} are tuning parameters for the logistic function, DD_{eff} represents the sum of effective

340 temperature for bark beetle reproduction in °C.Day^{-1}, while DD_{ref} denotes the thermal sum of degree days for one

341 bark beetle generation in °C.Day^{-1}. Saturation of $i_{beetles\,generation}$ represents the lack of available breeding substrate when

342 many generations develop over a short period.

343

344 DD_{eff} is calculated from January 1st until the diapause of the first generation. In ORCHIDEE, diapause is triggered

345 when daylength exceeds 14.5 hours (e.g., April 27th for France). Each day before the diapause with a daily average

346 temperature around the bark above 8.3°C (T_{min}) and below 38.4°C (T_{max}) is accounted for in the summation of DD_{eff}

347 (eq.10). This approach simulates the phenology of bark beetles, which tend to breed earlier when winter and spring

348 were warmer, thus allowing for multiple generations in the same year (Hlásny et al., 2021a).

349 $$DD_{eff} = \sum_{n_{diapause}}^{i=1} \left(T_{opt} - T_{min} \right) \cdot e^{\left(0.0288.\,T_{bark,i} \right)} - e^{\left(0.0288.\,b_{eff} - \left(40.99 - T_{bark,i} \right)/3.59 \right)} - 1.25 \quad (10)$$

350

351 Where i is a day, $n_{diapause}$ is the number of days between the 1st of january and the day of the diapause. T_{opt} $(30.3°C)$ is

352 the optimal bark temperature for beetles development and T_{min} $(8.3°C)$ is the temperature below which the beetles

353 developpement stop. $T_{bark,\,i}$ is the average daily bark temperature. $T_{bark,\,i}$ is calculated as the daily average air

354 temperature minus 2°C. All parameters values are taken from Temperli et al. 2013

355 The bark beetle activity of the previous year ($i_{beetles\,activity}$) is calculated as:

356

357 $$i_{beetles\,activity} = 1/\left(1 + e^{-S_{activity} \left(\frac{B_{kill,\,y-1}}{B_{total}} - ac\,t_{limit} \right)} \right) \qquad (11)$$

358

359 Where $i_{beetles\,activity}$ denotes the biomass of the stand damaged by bark beetles in the previous year, B_{total} is the total

360 biomass of the stand, and $S_{activity}$ and act_{limit} are parameters that drive the intensity of this negative feedback.

361

362 During the build-up stage the population of bark beetles can either return to its endemic stage if tree defense
363 mechanisms are preventing bark beetles from successfully attacking healthy trees, or evolve into an epidemic stage
364 (Fig. 1) if the tree defense mechanisms fail. During the post-epidemic stage, the forest is still subject to higher
365 mortality than usual but signs of recovery appear (Hlásny et al., 2021a). Recovery may help the forest ecosystem to
366 return to its original state or switch to a new state (different species, change in the forest structure) depending on the
367 intensity and the frequency of the disturbance (Van Meerbeek et al., 2021).
368

369 ### 2.7. Bark beetle survival
370 The capability of the bark beetles to survive the winter in between two breeding seasons is critical in simulating
371 epidemic outbreaks. During regular winters, winter mortality for bark beetles is around 40% for the adults and 100%
372 for the juveniles (Jönsson et al. 2012). In our scheme, this mortality rate is implicitly accounted for in the calculation
373 of the bark beetle survival index ($i_{beetles\ survival}$). A lack of data linking bark beetle survival to anomalous winter
374 temperatures, justifies the implicit approach and prevented including this information as a modulator of $i_{beetles\ survival}$.
375 The latter explains why winter temperatures do not appear in eq. 11. Instead the model simulates the survival as a
376 function of the abundance of suitable tree hosts which decreases the competition for shelter and food:
377

378 $$i_{beetles\ survival} = max\left(i_{hosts\ dead}, i_{hosts\ alive}\right) \qquad (12)$$

379

380 The availability of wood necromass from trees that died recently, particularly following windstorms, plays a critical
381 role in bark beetle survival and proliferation. In the year following a windstorm, uprooted and broken trees may offer
382 an ideal breeding substrate for bark beetles, facilitating their population growth.
383

384 In Temperli et al. (2013) an empirical correlation between windthrow events and bark beetle susceptibility was
385 established. ORCHIDEE enhances realism by considering the actual suitable hosts (living or recently dead trees) as
386 the primary driver of bark beetle survival. To avoid overestimating bark beetle population growth, max_{Nwood} has been
387 introduced. Any addition of dead trees beyond max_{Nwood} is considered ineffective in affecting the bark beetle
388 population. This ensures that an excess of breeding substrate does not artificially inflate beetle numbers.
389 This relationship is quantitatively represented in ORCHIDEE through the dead host index, $i_{hosts\ dead}$, which is driven
390 by the availability of recent dead trees. The formulation of $i_{hosts\ dead}$ is as follows:
391

392 $$i_{hosts\ dead} = min\left(\frac{N_{wood}}{B_{wood}} / max_{Nwood}, 1\right) \qquad (13)$$

393

394 Here, N_{wood} represents the quantity of woody necromass from the current year, B_{wood} is the total living woody biomass
395 in the stand, and max_{Nwood} is the threshold of the ratio N_{wood}/B_{wood} signifying the maximum level. This index captures
396 the immediate increase in dead trees suitable for bark beetle breeding following a windthrow event. However, it
397 takes about a year for dead wood to lose its freshness and suitability for bark beetle breeding. This is accounted for

398 by excluding woody necromass that is older than 1 year from the $i_{hosts\ dead}$ calculation.

399

400 max_{Nwood} can also be considered as a parameter that depends on the spatial scale of the simulation. The mortality rate

401 of trees ($DR_{windtrow}$) that will trigger an outbreak is very different across spatial scales. Where a relatively high share

402 of dead wood is needed to trigger an outbreak at the patch-scale, a much lower share of dead wood suffices at the

403 landscape-scale to trigger a widespread bark beetle outbreak. So these parameters must be set according to the

404 spatial resolution of the simulation experiment.

405

406 $i_{hosts\ alive}$ denotes the survival of bark beetles which is facilitated by the abundance of suitable trees which reduces the

407 competition among bark beetles for breeding substrates and therefore increases their survival.

408

409 $$i_{hosts\ alive} = i_{beetles\ mass\ attack} \times i_{hosts\ susceptibility} \qquad\qquad (14)$$

410

411 The amount of suitable tree hosts $i_{hosts\ alive}$ is driven by two factors: (1) the abundance of weak trees which can be

412 more easily infected by bark beetles. ORCHIDEE does not explicitly represent weak trees, but tree health is thought

413 to decrease with an increasing density given the stand diameter. The index for host suitability is thus calculated by

414 making use of the relative density index ($i_{rd\ spruce}$).

415

416 $$i_{hosts\ susceptibility} = 1/\left(1 + e^{S_{susceptibility} \cdot \left(i_{rd\ spruce} - i_{rd\ susceptibility}\right)}\right) \qquad\qquad (6a')$$

417

418 Equation 6a' is close to equation 6a but the parameter $S_{susceptibility}$ has been reduced by a factor of two in order to

419 reflect that $i_{hosts\ susceptibility}$ is more sensitive to $i_{rd\ spruce}$ than $i_{hosts\ competition}$. (2) $i_{hosts\ mass\ attack}$ which represent the ability of bark

420 beetles to attack healthy trees when the number of bark beetles is large enough. This index only depends on the size

421 of the bark beetle population ($i_{beetles\ pressure}$ see eq. 8)

422

423 $$i_{hosts\ mass\ attack} = 1/\left(1 + e^{S_{mass\ attack} \cdot \left(i_{beetles\ pressure} - B\,P_{limit}\right)}\right) \qquad\qquad (15)$$

424

425 Where $S_{hosts\ mass\ attack}$ and BP_{limit} are parameters. $S_{mass\ attack}$ controls the steepness of the relationship while BP_{limit} is the

426 bark beetle pressure index at which the population is moving from endemic to epidemic stage where mass attacks are

427 possible.

428

429 The epidemic stage corresponds to the capability of bark beetles to mass attack healthy trees and overrule tree

430 defenses (Biedermann et al., 2019). At this point in the outbreak, all trees are potential targets irrespective of their

431 health. Three causes have been suggested to explain the end of the epidemic phase: (1) the most likely cause is a

432 high interspecific competition among beetles for tree host when the density is decreasing (decreasing $i_{hosts\ alive}$)

433 (Komonen et al., 2011; Pineau et al., 2017), (2) a series of very cold years will decrease their ability to reproduce

434 (decreasing $i_{beetles\,generation}$), and (3) a rarely demonstrated increasing population of beetle predators (Berryman, 2002).

435 In ORCHIDEE r8627, the first two causes are represented but the last, i.e. the predators are not.

436

2.8. Tree mortality from bark beetle infestation

438 When bark beetles attack a tree, the success of their attack will likely depend on the capability of the tree to defend

439 itself from the attack. Trees defend themselves against beetle attacks by producing secondary metabolites (Huang et

440 al., 2020). The high carbon and nitrogen costs of these compounds limit their production to periods with

441 environmental conditions favorable for growth (Lieutier, 2002). The probability of a successful bark beetle attack is

442 driven by the size of the bark beetle population ($i_{beetles\,pressure}$) and the health of each tree. ORCHIDEE, however, is not

443 simulating individual trees but rather diameter classes within an age class. An index of tree health for each age class

444 ($i_{hosts\,health,\,age\,class}$) was calculated as:

445

446 $$P_{success,\,age\,class} = i_{hosts\,health,\,age\,class} \times i_{beetles\,pressure} \qquad (16)$$

447

448 A tree rarely dies solely from bark beetle damage (except during mass attacks) as female beetles often carry blue-

449 stain fungi, which colonizes the phloem and sapwood, blocking the water-conducting vessels of the tree (Ballard et

450 al., 1982). This results in tree death from carbon starvation or desiccation. As ORCHIDEE r8627 does not simulate

451 the effects of changes in sapwood conductivity on photosynthesis and the resultant probability of tree mortality, the

452 index of weakened trees index ($i_{hosts\,health,\,age\,class}$) makes use of two proxies similarly to equation 5 and 6 but simplified

453 to be calculated only for one age class at a time:

454

455 $$i_{hosts\,health,\,age\,class} = \frac{\left(i_{hosts\,competition,\,age\,class} + i_{hosts\,defense,\,age\,class}\right)}{2} \qquad (17)$$

456

457 $$i_{hosts\,defense,\,age\,class} = 1/\left(1 + e^{S_{drought}\cdot\left(1 - PW\,S_{age\,class} - PW\,S_{limit}\right)}\right) \qquad (5a')$$

458

459 Contrary to equation 5a, $PWS_{age\,class}$ is the plant water stress from the current year.

460

461 $$i_{hosts\,competition,\,age\,class} = 1/\left(1 + e^{S_{competition}\cdot\left(i_{rd\,age\,class} - i_{rd\,limit}\right)}\right) \qquad (6a'')$$

462

463 $$i_{rd\,age\,class} = \frac{D_{age\,class}}{D_{max}} \qquad (6b'')$$

464

465 To access the bark beetle damage rate ($DR_{beetles}$), $B_{beetles\,kill}$ has to be divided by B_{total}.

466

467

468   **2.9.**   **Flow of the calculations**

469 The equations presented above contain feedback loops which have been visualized in Fig. 2. In ORCHIDEE these

470 feedback loops are accounted for in subsequent time steps rather than the same time step.
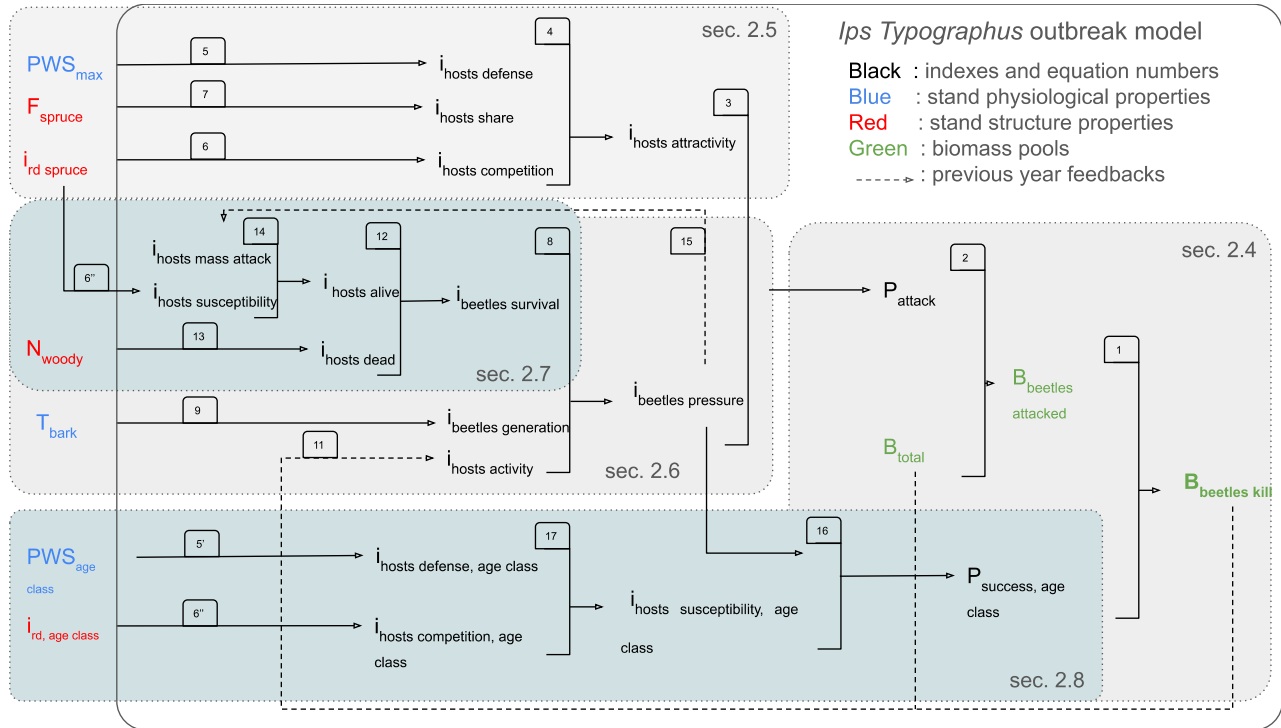
471

Figure 2: Order of the calculations and feedback in the *Ips typographus* outbreak model of ORCHIDEE. The numbers correspond to the equation numbers in this study. The dotted line boxes represent 5 main concepts of the outbreak model described in section 2.4, 2.5, 2.6, 2.7, 2.8.

472

473 **3.**   **Methods and material**

474   **3.1.**   **Model configuration**

475 Given the large-scale nature of the ORCHIDEE, a sensitivity experiment of the bark beetle outbreak functionality

476 was carried out rather than focusing the model evaluation on matching observed damage volumes at specific case

477 studies. Focussing on model sensitivity for a range of environmental conditions is thought to reduce the risk of

478 overfitting the model to specific site conditions (Abramowitz et al., 2008).

479

480 ORCHIDEE r8627 including the bark beetle model was run at the location of eight FLUXNET sites, selected to

481 simulate a credible temperature and precipitation gradient for spruce (see below). For each location, the half-hourly

482 meteorological data from the flux tower were gap filled and reformatted so that they could be used as climate forcing

483 by the ORCHIDEE. Boundary conditions for ORCHIDEE, such as soil texture, pH and soil color were retrieved

484 from the USDA map, for the corresponding gridcell. The observed land cover and land use for the gridcell were

485 ignored and set to pure spruce because this study did not investigate the effect of species mixture in the simulation

486 experiments. The resolution of the gridcell chosen for this analysis is 2500 km². Although this corresponds to a high

487 resolution for large-scale simulations with ORCHIDEE it is a coarse resolution for studying bark beetle outbreaks.

488

489 The climate forcings were looped over as much as needed to bring the carbon, nitrogen, and water pools to

490 equilibrium during a 340 years long spinup. Following the spinup, a 100-years simulation was run starting with a

491 windthrow event on the first day of the first year. The results presented in this study come from the 100-years long

492 simulations. Given the focus on even-aged monospecific spruce forests in regions where spruce growth is not

493 constrained by precipitation, variables such as $i_{hosts\ share}$ and $i_{hosts\ defense}$ were omitted from this study. Note that

494 ORCHIDEE does not account for possible acclimation e.g., temporal changes in bark beetle behavior or bark beetle

495 resistance to external stressor such as winter temperature.

496

497   **3.2.   Selection of locations**

498 Bark beetle populations are known to be sensitive to temperature as they are more likely to survive a mild winter

499 (Lombardero et al., 2000) and tend to breed earlier when winter and spring are warmer than usual, allowing for

500 multiple generations in the same year (Hlásny et al., 2021a, also see eq. 10 from section 2.6). In order to assess the

501 temperature effect of the bark beetle outbreak model in ORCHIDEE, eight locations in Europe were selected (Table

502 2) which represent the range of climatic conditions within the distribution area of Norway spruce (*Picea Abies* Karst

503 L.), the main host plant for *Ips typographus,* the bark beetle species under investigation.

504

Table 2: Climate characteristics of the eight locations used in the simulation experiments. The acronyms refer to the site names used in the FLUXNET database (Pastorello et al. 2020).

Site	FI-HYY	DK-SOR	DE-THA	CZ-WET	FR-HES	FR-FON	IT-REN	IT-COL
Full name	Hyytiala	Soroe	Tharandt	Třeboň	Hesse	Fontainebleau	Renon	Collelongo
Country	Finland	Denmark	Germany	Czech	France	France	Italy	Italy
Latitude (°N)	61.84	55.49	50.96	49.02	48.4	48.48	46.59	41.85
Longitude (°E)	24.29	11.64	13.57	14.77	7.1	2.78	11.43	13.59
MAT (°C)	3.8	8.2	8.2	7.7	9.5	10.2	4.7	6.3
MinAT (°C)	-10.8	2.7	-3.9	-5.2	0.1	-1.1	-6.3	-3.8
MAP (mm.y^{-1})	522	811	734	587	653	989	752	1050
Mean annual net radiation (w.m^{-2})	42.1	49.4	52.5	68.0	53.7	50.3	67.7	68.3

505 For these eight locations, half-hourly weather data from the FLUXNET database (Pastorello et al., 2020) were used

506 to drive ORCHIDEE. Some of these locations (FON, SOR, HES, COL, WET) are in reality not covered by spruce

507 but all sites are, however, located within the distribution of Norway spruce. In this study, locations were selected to

508 use the observed weather data to simulate a credible temperature and rainfall gradient for spruce. HES location is no

509 longer part of the FLUXNET network but the previous data are still available are relevant for this analysis.

510

511   **3.3.   Sensitivity to model parameters**

512 The sensitivity assessment evaluates the responsiveness of four key variables ($i_{hosts\ susceptibility}$, $i_{beetles\ mass\ attack}$, $i_{beetles\ generation}$,

513 $i_{beetles\ activity}$) of the *Ips typographus* outbreak model implemented in ORCHIDEE. The assessment aims to demonstrate

515 the ability of ORCHIDEE to simulate diverse dynamics of bark beetle infestations. The selection of $i_{hosts\ susceptibility}$,

516 $i_{beetles\ activity}$, $i_{beetles\ mass\ attack}$, and $i_{beetles\ generation}$ was based on two criteria: (1) their substantial influence on the dynamics of

517 the *Ips typographus* outbreak noted during model development, and (2) their independence from direct measurable

518 data, rendering them less suitable for evaluation through literature review.

519

520 For each of the four variables, three distinct values were assigned to two parameters labeled "Shape" and "*Limit*".

521 The *Shape* parameter determines the shape of the logistic relationship, with three values tested: (a) *Shape=-1.0*,

522 yielding a linear relationship, (b) *-5.0<Shape<-30.0,* resulting in a logistic curve, and (c) *Shape=-500.0*, turning the

523 logistic relationship into a step function. For the logistic curve, the exact *Shape* value between -30.0 and -5.0 is

524 chosen according to each index under study: (1) $S_{susceptibility}$ = -5.0; (2) $S_{activity}$= -20.0; (3) $S_{mass\ attack}$= -30.0; and (4)

525 $S_{generation}$=5.0 . For $S_{mass\ attack}$ and $S_{activity}$, higher values have been chosen because the slope of the logistic curve has a

526 significant impact in order to trigger an outbreak.

527

528 The second parameter called "*Limit*" determines the threshold, derived from expert insights, at which the logistic

529 relationship will reach its midpoint value of 0.5 ($i_{rd\ susceptibility}$, BP_{limit}, Act_{limit}, *or* G_{limit}). For instance, $i_{rd\ susceptibility}$ is set at

530 0.55, indicating $i_{hosts\ susceptibility}$ midpoint sensitivity (Eq. 6'). Setting BP_{limit} at 0.12 results in an $i_{beetles\ mass\ attack}$ midpoint

531 when $i_{beetles\ pressure}$ is 0.12, selected for its proximity to scenarios where $i_{hosts\ dead}$ equals 1.0 (Eq. 14). Act_{limit}, was

532 positioned at 0.06, signifying the $i_{beetles\ activity}$ midpoint at a $DR_{beetles}$ = *6%* from the preceding year, exceeding endemic

533 levels yet not reaching epidemic outbreaks (Eq. 10). Lastly, G_{limit} is fixed at 1.0, denoting the midpoint for $i_{beetles}$

534 $_{generation}$ upon completing one generation annually, underpinning the rarity of bark beetle outbreaks with fewer than

535 one generation per year (Eq. 9). Starting from these reference values, a "*restrictive*" simulation was run in which the

536 "*Limit*" parameter values were reduced by 50%. Likewise a "*permissive*" simulation was run to test 50% higher

537 values for "*Limit*".

538

539 The sensitivity analysis of the model parameters explores 36 (3 shapes x 3 limits x 4 equations) combinations of

540 parameters values named "set", but the full design of the experiment is 8^3=512 sets (8 parameters, 3 values for each).

541 This deliberate choice has been made because of the computation time cost of a single run. In order to reduce the

542 number of runs from 512 to 36, we had to make simplifications: (1) one equation at the time is studied, reducing to 9

543 the number of sets necessary to realize the sensitivity analysis (2) every other parameters from the remaining

544 equation is set to default value e.g. "Limits" are set to their reference values and "shape" are set to their a priori

545 assumption (table 4). The major drawback of this approach is that interaction effects between equations can not be

546 investigated in the study. Nonetheless, this sensitivity analysis aims to document model behavior, rather than seeking

547 precise parameter values which can be achieved with the main effect of each equation only (see section 3.4).

548 The simulations were run for the THA site, where they were repeated for two prescribed windthrow events with a

549 different intensity, i.e., a $DR_{windthrow}$ of 0.1 and 10%. The effect of the parameters with a negligible windthrow event,

550 i.e., killing only 0.1% of the trees, was tested to confirm that the selected parameters did make ORCHIDEE simulate

551 a bark beetle outbreak in the absence of windthrow (*score5* in section 3.4).

3.4. Parameter tuning and credibility score

The results of the sensitivity experiment were used to select key model parameters. Selecting the values for the *Shape* and *Limit* parameters (see section 3.3) used in the calculation of the variables $i_{hosts\ susceptibility}$, $i_{beetles\ mass\ attack}$, $i_{beetles\ generation}$, and $i_{beetles\ activity}$ has been carried out in order to reproduce the observed dynamics of bark beetle outbreaks. Observed dynamics were compiled through a literature search for peer-reviewed papers that reported quantitative characteristics of bark beetle outbreaks (Table 3). Four characteristics could be documented and use to calculate score:

- The delay between the windthrow event and the start of the bark beetle outbreak (*score1*).
- The length of the bark beetle outbreak is defined by the number of years required for a bark beetle population to go back to its endemic level (*score2*).
- The cumulative number of trees per unit area, killed by the bark beetles at the end of an outbreak (*score3*).
- The average tree mortality rate ($DR_{beetles}$) during an endemic stage (*score4*).

Based on Table S1 and the reference range in Table 3, scores are calculated for each parameter set. The Credibility Score (*CS*) is the sum of four scores, indicating that the result falls within the four reference ranges described above and no outbreak is triggered when DRwindthrow = 0.1%. The *CS* is computed as follows: *CS = (score1 + score2 + score3 + score4) x score*5. Only parameter sets achieving a *CS* of 4 will be selected. If multiple parameter values are possible for a given equation, the most frequently selected value will be preferred.

Table 3 : Literature-based summary of characteristics of large-scale bark beetle outbreaks. Due to data spacity, the characteristics combine outbreak dynamics of different bark beetle species, different host species, and different locations. The reference range is used to calculate the credibility score (CS) of each set of parameters (but see table s1).

Outbreak characteristics	Literature findings	Reference range	How to estimate in ORCHIDEE ?
Delay before the start of an outbreak (build-up)	A notable surge in the population of *I. typographus* was observed in windthrow areas during the second to third summer following the storm (Havašová et al., 2017; Kärvemo and Schroeder, 2010; Wermelinger, 2004; Wichmann and Ravn, 2001).	[2, 3] years, use in the calculation of *score1*	Using the tree mortality rate by bark beetles ($DR_{beetles}$), one can access the number of years since the storm before reaching the maximum mortality rate (epidemic stage).
Length of an outbreak (epidemic)	Studies suggest that *I. typographus* outbreaks in Europe can last anywhere from 11 to 17 years (Bakke, 1989; Hlásny et al., 2021b; Mezei et al., 2014).	[11, 17] years, use in the calculation of *score2*	Using the tree mortality rate by bark beetles ($DR_{beetles}$), one can access the number of years past since the storm before reaching the minimum mortality rate (endemic stage).
Severity rate of an outbreak (severity)	A severe bark *D. Ponderosa* outbreak resulted in a 52%-60%	Highly dependent from the size of the forest studied	Count the number of trees killed by bark beetles until the end of the

	reduction in tree numbers at large landscape scale (>2000km²) (Morehouse et al., 2008; Pfeifer et al., 2011) In Wallonia and East France, *I. Typographus* outbreak resulted in 12.6% reduction of spruce forest area in 6 years (Arthur, G., et al. 2024).	but for a grid cell of 2500km2, ones could expect a [25%, 45%] reduction over the entire course of a massive outbreak. Use in the calculation of *score3*	outbreak, then divide by the number of trees just after the storm event.
Endemic mortality rate (endemic)	Total background mortality is around 1.2%.year^{-1}. Bark beetles as a functional group are estimated to account for 40% of the total mortality in the United States (≈0.5%.year^{-1}) (Berner et al., 2017; Das et al., 2016; Hlásny et al., 2021b).	Not enough data was available to estimate a range. Nonetheless we decided to calculate a range including a 10% uncertainty [0.45-0.55] %.year^{-1}. Use in the calculation of *score4*	After the end of the outbreak, count the number of trees that die every year. Then average it.

572

3.5.   Sensitivity to climate and windthrow

574 In this simulation experiment, the influx of fresh dead tree hosts (N_{wood}) used for bark beetle breeding was controlled
575 by modifying the maximum damage rate of a windthrow event ($DR_{windthrow}$) in ORCHIDEE. Seven $DR_{windthrow}$ were
576 simulated (i.e, 0.1%, 5%, 7.5%, 10%, 15%, 20%, 35%). Given the monotonic nature of the relationships between
577 $DR_{windthrow}$ and $i_{hosts\ dead}$ (Eq. 12), each event triggers a proportional increase in the dead host availability ($i_{hosts\ dead}$)
578 scaling between 0 and 1 (Fig. 3). Through its equations, ORCHIDEE assumes that for damage rates above 20% the
579 variable $i_{hosts\ dead}$ (N_{wood}) will always be equal to 1.0. $i_{rd\ spruce}$, however, may further decrease with increasing windthrow
580 damage, which makes the 35% damage rate still interesting to investigate. Although the simulations were run for all
581 $DR_{windthrow}$, only four windthrow damage rates including a windstorm resulting in a 35% damage rate (Fig. 3), were
582 presented to enhance the readability of the result section.

583
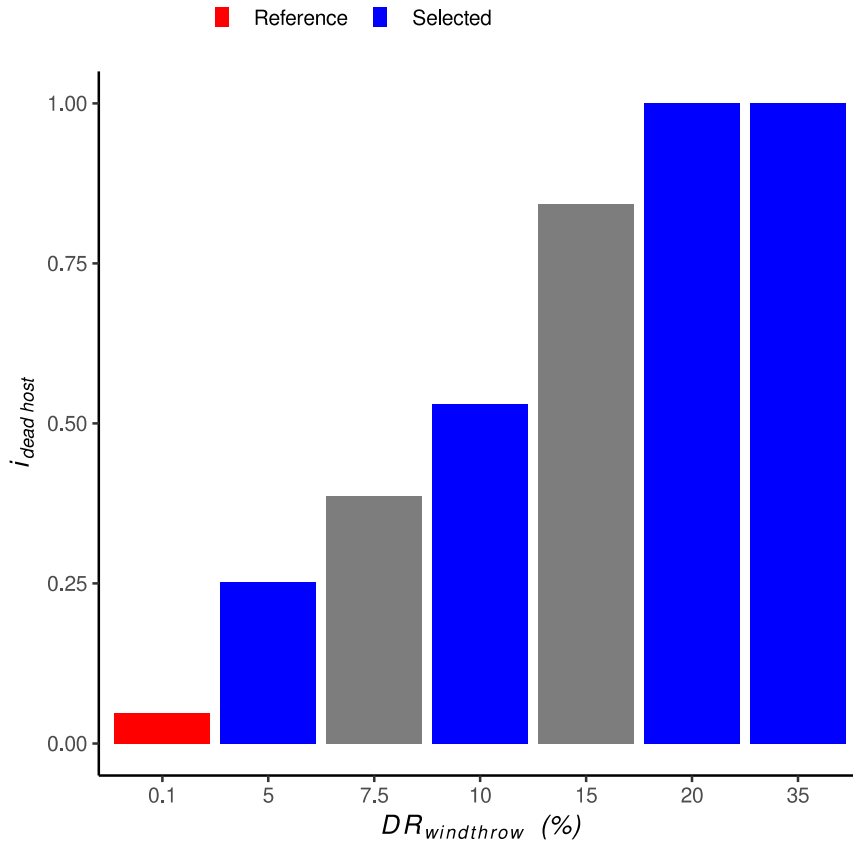
Figure 3: Relationship between windthrow damage rate ($DR_{windthrow}$) and dead host index ($i_{hosts\ dead}$). For each site a $DR_{windtrow}= 0.1\%$ was used as the reference simulation because an endemic bark beetle population is expected following such a low intensity windthrow event. The four $DR_{windthrow}$ shown in blue were selected for subsequent presentation of the results because they cover the entire range for the $i_{hosts\ dead}$.

The main driver of the number of generations a bark beetle population can achieve in one year is the number of days higher than 8.3°C during winter time (Temperli et al., 2013) which is the reason why temperature is so important for bark beetle reproduction. By taking REN, THA, WET and HES, the number of bark beetle generations ranged from 0.8 to 3.5 (Fig. 4) which is similar to the number of generations observed across Europe (Faccoli and Stergulc, 2006; Jönsson et al., 2009, 2011). Limiting the analysis to only four sites simplifies the presentation without affecting the range under investigation.
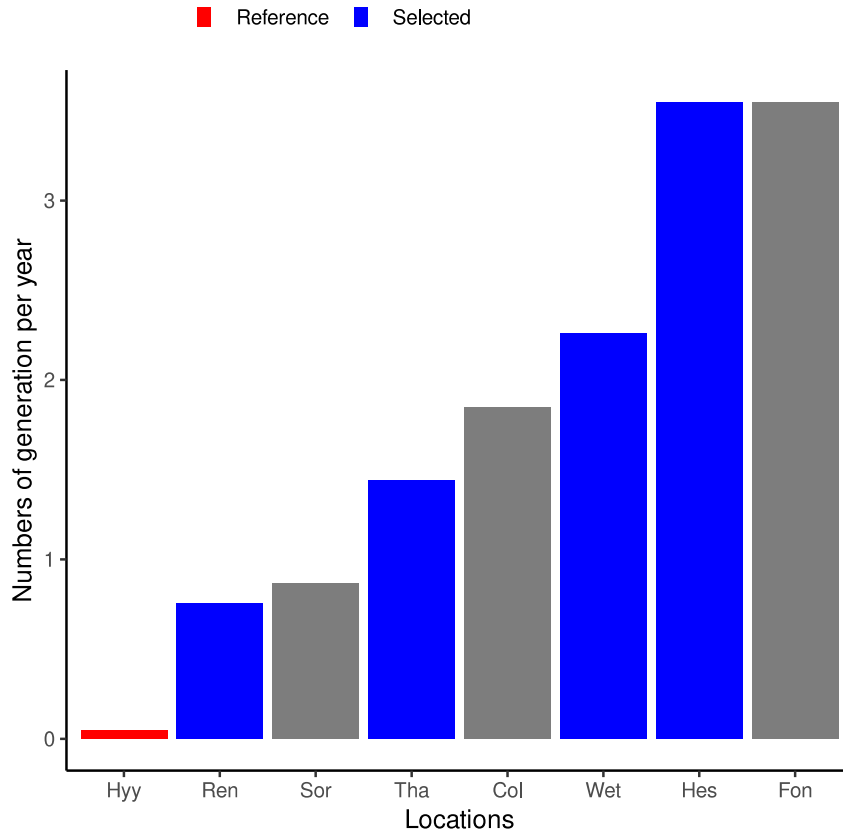
Figure 4: Average number of bark beetle generations during the 5 years following the wind storm for at eight locations along a climate gradient. The HYY location in Finland was selected as the reference for the REN, THA, WET and HES locations. Only results from the reference and four selected locations (shown in blue) are shown in the results to enhance readability.

591

592 For the climate gradient, the simulation for HYY served as a reference since the number of generations is lower than
593 1 for which no outbreak should happen under any circumstances. Under present climate conditions, an outbreak in
594 HYY should be considered an undesirable model result. Likewise, a $DR_{windthrow}=0.1\%$ is considered too low to trigger
595 an outbreak and was therefore used as the reference for the wind damage rate tests.

596

597 The experiment consisted of 40 simulations, i.e., 8 sites (including the reference) x 5 wind damage rates (including
598 the reference). Although the simulations were also run for SOR, COL and FON their results were found to be too
599 similar to the results of selected sites to present them as well. Hence, the result section presents only 25 out of the 40
600 simulations. Three output variables were assessed: bark beetle damage rate ($DR_{beetles}$), total biomass (B_{total}), and net
601 primary production (NPP). Total biomass was investigated over 100 years whereas $DR_{beetles}$ and NPP were assessed
602 for the first 20 years following a windthrow.

603

3.6. Continuous vs abrupt mortality

Where most land surface models use a fixed turnover time to simulate continuous mortality (Pugh et al., 2017; Thurner et al., 2017), ecological reality is better described by abrupt mortality events. An idealized simulation experiment was used to qualify the impact of abrupt mortality on net biome productivity by changing from a framework in which mortality is approximated by a constant background mortality to a framework in which mortality occurs in abrupt, discrete events. The impact of a change in mortality framework was assessed with an idealized simulation experiment that compares three configurations of ORCHIDEE: (1) a configuration that simulates mortality as a continuous process, labeled "the continuous configuration" which corresponds to previous versions of ORCHIDEE, and (2) a configuration capable of simulating abrupt mortality from windthrow and subsequent bark beetle outbreaks, labeled "the abrupt configuration" and (3) a configuration in which windthrow is activated but bark beetles outbreak is implicitly accounted for in the background mortality. This third configuration enabled attributing the impact to windthrow. The effect of simulating abrupt mortality was evaluated over 20, 50, and 100 year time horizons.

The impact of changing the mortality framework from continuous to abrupt was quantified on the basis of 120 simulations (8 locations x 7 windthrow damage rates x 2 configurations + 8 sites x 1 configuration) of 100 years each.

The simulations with abrupt mortality were run first. Subsequently, the number of trees killed was quantified and used as a reference value for the continuous mortality set-up. This approach resulted in the same quantities of dead trees at the end of the simulation for both frameworks, which then differed only in the timing of the simulated mortality. This precaution is necessary to avoid comparing two different mortality regimes where the result would mainly be explained by the intensity of the mortality rather than by its underlying mechanisms.

Changes in forest functioning were evaluated through the temporal evolution of accumulated net biome productivity (*NBP*) over a 100-years time frame. *NBP* is defined as the regional net carbon accumulation after considering losses of carbon from fire, harvest, and other episodic disturbances. In ORCHIDEE, *NBP* is calculated following the definition by Chapin et al. (2006) as the carbon remaining in the biomass, litter and soil after accounting for photosynthesis, and respiration because fire, harvest, leaching and volatile emissions were not accounted for in this simulations experiment.

4. Results
4.1. Sensitivity to model parameter sets

The impact of spruce stand competition ($i_{hosts\ susceptibility}$) on outbreak dynamics was examined by adjusting the parameters $S_{susceptibility}$ and $i_{rd\ susceptibility}$ in equation 6a'. When $S_{susceptibility}$ resulted in a linear relationship ($S_{susceptibility}$ = -*1.0*), no peak in bark beetle damage occurred for the three tested values of $i_{rd\ susceptibility}$ (permissive, reference, restrictive) at a 10% windthrow damage rate (Fig. 5, panel h). However, employing a step function *($S_{susceptibilty}$ = -*

641 *500.0*) led to either sporadic peaks of bark beetle damage with a permissive $i_{rd\ susceptibility}$ or a two-year outbreak with a

642 maximum damage rate of 60% with a restrictive $i_{rd\ susceptibility}$ (Fig. 5, panel h), neither of which aligns with the

643 observations summarized in Table 3.

644

645 The closest outcome to observation from table 3 was obtained with a logistic relationship ($S_{susceptibility}$ = *-5.0*), where

646 $i_{rd\ susceptibility}$ determined the duration of the outbreak: 11, 16, and 25 years for restrictive, reference, and permissive

647 parameter values, respectively (Fig. 5, panel h). Either the restrictive or reference parameter value could be utilized

648 since a range of 11-16 years aligns with the observations (Table 3). To examine the occurrence of improbable

649 outbreaks, sensitivity tests were repeated for a 0.1% windthrow damage rate. None of the nine parameter

650 combinations triggered an outbreak (Fig. 5, panel g), suggesting that improbable outbreaks due to the calculation of

651 $i_{hosts\ susceptibility}$ are unlikely.

652

653 From the calculation of the credibility score, only one set obtains a score of 4 ($S_{susceptibility}$ = *-5.0, $i_{rd\ susceptibility}$=0.55*,

654 Table s1). The concerning parameters value has been selected and reported in table 4.

655

656 The effect of the capability of bark beetle to mass attack ($i_{beetles\ mass\ attack}$) when the population exceeds a threshold was

657 evaluated by varying $S_{mass\ attack}$ and BP_{limit} (Eq. 14). Linear relationships ($S_{mass\ attack}$ = -1.0) resulted in similar outbreak

658 dynamics for all BP_{limit} values, with the model settling on a constant endemic damage following an outbreak, though

659 higher than observed (Table 3, Fig. 5, panel f). Introducing a logistic or step function slightly altered outbreak

660 dynamics except when assuming a step function for the restrictive value, which prevented an outbreak. Repeating

661 sensitivity tests for a 0.1% windthrow damage rate showed that assuming linear or logistic relationships could trigger

662 an outbreak (Fig. 5, panel e), indicating that improbable outbreaks may arise from the calculation of $i_{hosts\ mass\ attack}$.

663

664 From the calculation of the credibility score, three sets obtain a score of 4 but only set 4.6 was chosen because of its

665 intermediate position compared to sets 4.9 and 4.5 (Table s1). The concerning parameter values ($S_{mass\ attack}$ = *-30.0*,

666 BP_{limit}=*0.06*) have been selected and reported in table 4.

667

668 The impact of bark beetle activities from the previous year ($i_{beetles\ activity}$) on outbreak dynamics was investigated by

669 varying $S_{activity}$ and act_{limit} (Eq. 10). Linear or logistic relationships resulted in excessively long outbreaks (>30 years)

670 compared to observations (Table 3, panel b), whereas assuming a step-function relationship simulated a decline in

671 the outbreak after 14 years. Sensitivity tests repeated for a 0.1% windthrow damage rate showed that assuming a

672 linear relationship could trigger an improbable outbreak (Fig. 5, panel a) through the calculation of $i_{beetles\ activity}$.

673

674 From the calculation of the credibility score, only one set obtains a score of 4 ($S_{activity}$ = *-500.0, act_{limit}=0.12*, Table

675 s1). The concerning parameters value has been selected and reported in table 4.

676

677 To explore the effect of the numbers of generation ($i_{beetles\ generation}$) on the outbreak dynamics, $S_{generation}$ and G_{limit} from

678 equation 9 were varied. Bark beetle damage rate was more sensitive to G_{limit} than $S_{generation}$, but only a linear

679 relationship with the reference $G_{limit} = 1.0$ yielded an intermediate outbreak intensity consistent with the continental

680 climate at the test location (i.e., THA, Fig. 5, panel d). Other combinations resulted in either too strong or no peak

681 during the outbreak. Repeating sensitivity tests for a 0.1% windthrow damage rate showed that none of the nine

682 parameter combinations triggered an outbreak (Fig. 5 panel c), indicating that improbable outbreaks from the

683 calculation of $i_{beetles\ generation}$ are unlikely.

684

685 From the calculation of the credibility score, three sets obtain a score of 4 but only set 1.4 was chosen because of its

686 intermediate position compared to sets 1.1 and 1.5 (Table s1). The concerning parameter values ($S_{generation} = 1.0$,

687 $G_{limit}=1.0$) have been selected and reported in table 4.
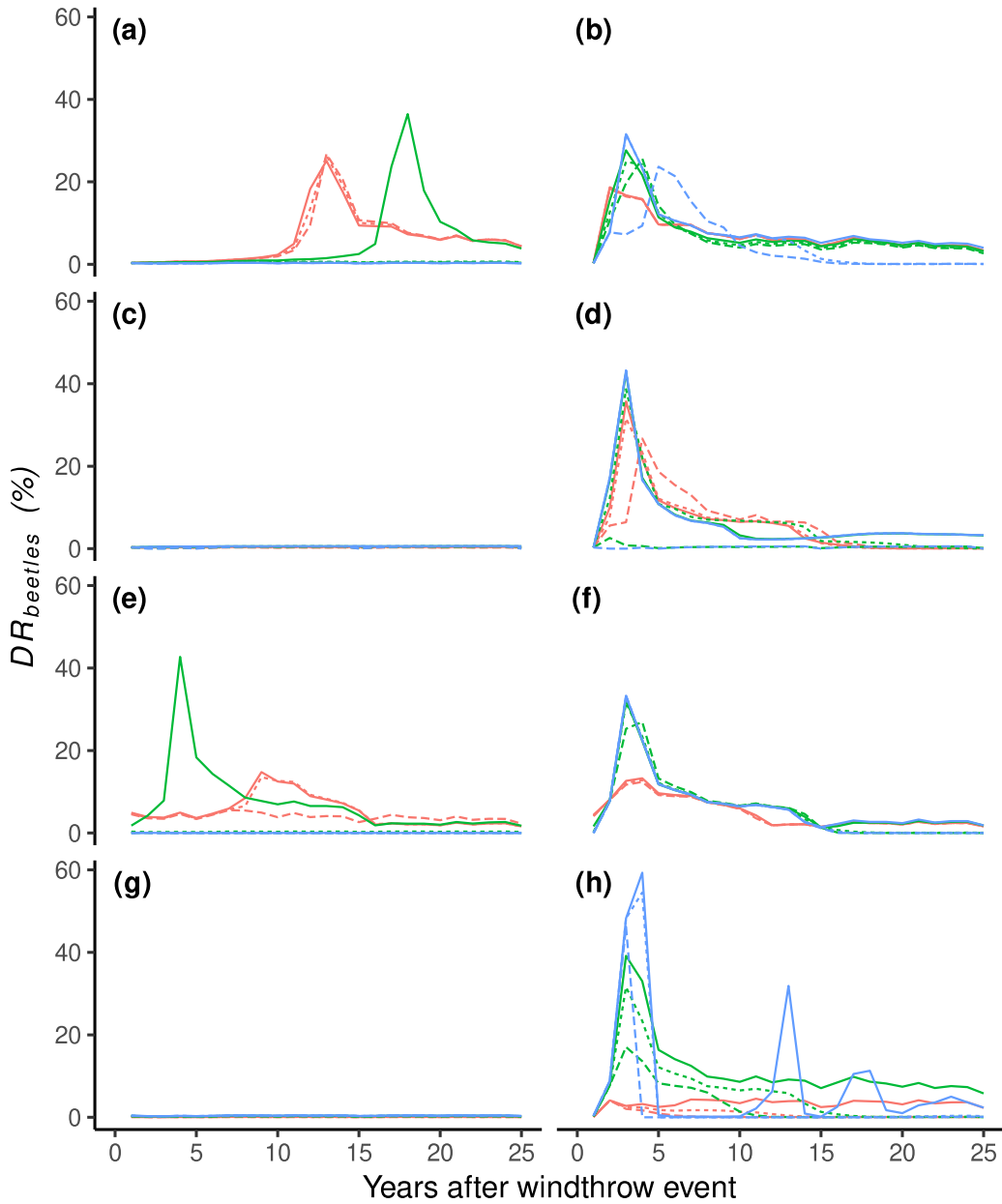
Figure 5: Simulation results from the sensitivity experiment at the THA site. Eight parameters from four equations were evaluated. Each equation represents an index from the bark beetle outbreak model ($i_{hosts\ susceptibility}$ $i_{hosts\ mass\ attack}$, $i_{beetles\ activity}$, $i_{beetles\ generation}$). Each index is represented by a logistic function defined by a shape parameter (*Shape*) and a limit parameter (*Limit*). Three values were chosen for each parameter resulting in 9 pairs of parameters for each index. Colored lines represent the shape parameter varying from linear : *Shape* = -1.0 (red), logistic -5.0 < *Shape* < -30.0 (green), to step function where *Shape* = -500.0 (blue). Line type represents three different values for *Limit* parameters where references (dashed line) are values of $i_{rd\ susceptibility}$, BP_{limt}, act_{limit} and G_{limit} (given in table 4), whereas permissive (full line) and restrictive (dashed dotted) represent a 50% decrease or increase respectively.

688

689 **4.2. Model tuning**

690 By comparing the outcomes of the sensitivity tests (section 4.1) to a compilation of observations (Table 3), a first

691 estimate for several parameters was proposed (Table 4).

692

Table 4: Parameter values from the bark beetle model based on the score obtained in the sensitivity analysis. (*) parameter values deliberately fixed and excluded from the sensitivity analysis (section 3.3 for justification).

Parameter	Source	Chosen parameters
$S_{generation}$	This study: from SA (see 3.1.4)	-1.0
G_{limit}	Adapted from Temperli et al. 2013	1.0
DD_{ref}	Adapted from Temperli et al. 2013	547.0 (*)
$S_{drought}$	Adapted from Temperli et al. 2013	-9.5 (*)
PWS_{limit}	Adapted from Temperli et al. 2013	0.4 (*)
max_{Nwood}	This study: scale dependent (see 2.4.2)	0.2 (*)
$S_{activity}$	This study: from SA (see 3.1.3)	-500.0
act_{limit}	This study: from SA (see 3.1.3)	0.06
$S_{susceptibility}$	This study: from SA (see 3.1.1)	-20.0
$i_{rd\ susceptibility}$	This study: from SA (see 3.1.1)	0.55
$S_{competition}$	This study: from SA (see 3.1.1)	-5.0 (*)
$i_{rd\ limit}$	This study: scale dependent (see 2.4.1)	0.4 (*)
$S_{mass\ attack}$	This study: From SA (see 3.1.2)	-30.0
BP_{limit}	This study: scale dependent (see 3.1.2)	0.12
S_{share}	This study: not used (see 2.5)	15.5 (*)
SH_{limit}	This study: not used (see 2.5)	0.6 (*)

693

694 **4.3. Impact of climate and windthrow on bark beetle damage**

695 In ORCHIDEE, the warmest sites, HES and WET, experienced significant bark beetle outbreaks across a wide

696 spectrum of windthrow mortality rates, whereas colder sites like REN and THA saw outbreaks only in response to

697 the most severe windthrow events (Fig. 6, panel b, c). A greater average number of bark beetle generations in the

698 years following windthrow events led to higher bark beetle damage rates at the peak of outbreaks. For instance, at a

699 35% windthrow mortality rate, HES reached a maximum bark beetle damage rate of 50%, whereas REN's maximum

700 was 22% (Fig. 6 panel a, b).

701

702 Interestingly, high tree mortality rates from windthrow could also lead to delays and lower maximum $DR_{beetles}$ (Fig.

703 6). For instance, at the HES site, 10%, 20%, and 35% windthrow damage rates triggered maximum $DR_{beetles}$ of 50%,

704 43%, and 37%, respectively (Fig. 6 panel a). Conversely, low $DR_{windthrow}$, like 5% at WET, delayed the peak of bark

705 beetle outbreaks by 9 years (Fig. 6, panel d). Additionally, the model simulated a post-epidemic stage during which

706 the outbreak damage rate remained relatively low (<10%) and lasted between 3 to 10 years (Fig. 6). Overall, the

707 simulated outbreaks lasted between 11 to 20 years, consistent with field observations (Table 3).
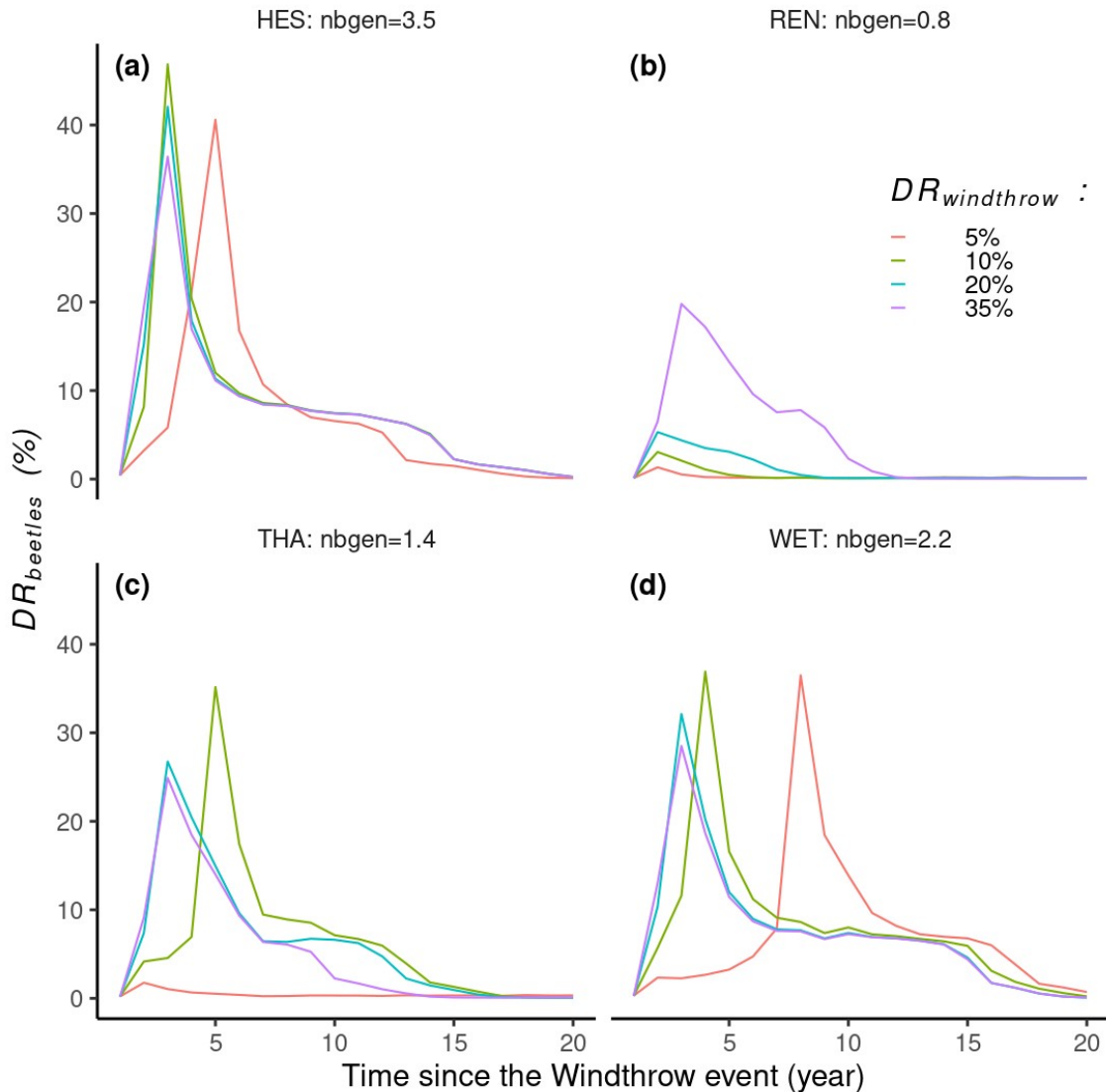
708

Figure 6: Simulation results of 16 simulations (4 locations x 4 windthrow damage rates $DR_{windthrow}$). Lines represent the annual bark beetle damage rate as a fraction of the total biomass ($DR_{beetles}$). *Nbgen* is the average number of bark beetle generations during five years after the windthrow event. $DR_{windthrow}$ represents the percentage of biomass loss by a windthrow event at the start of the simulation.

At the coldest site, HYY, ORCHIDEE simulated only a small number of bark beetle generations, preventing outbreaks from occurring. This observation validates the initial parameter tuning (Table 4), indicating that it is robust enough to prevent improbable outbreaks, such as the model triggering outbreaks in sites where bark beetles cannot reproduce.

4.4. Impact of climate and windthrow on stand biomass and Net Primary Production

All locations experienced a 10 to 20 years decrease in total biomass until at most 9 kgC.m^{-2} at which time the outbreak ended (Fig. 7, panel a, b, c, d). The model can simulate significant epidemic events even if the initial

28

718 trigger, such as the windthrow event in our study, is not particularly intense. Once the bark beetles can mass attack
719 living trees, the bark beetle population ($i_{beetles\ pressure}$) will increase and kill more and more trees until so many trees are
720 killed that the stand density of the remaining living trees drops below the threshold of $i_{rd\ spruce} = i_{rd\ limit}=0.4$. In
721 ORCHIDEE, an $i_{rd\ limit}=0.4$ for spruce forest corresponds to a biomass of around 9 kgC.m^{-2} which in ORCHIDEE is
722 too low to maintain an epidemic population of bark beetles at the 2500 km2 grid cell. Interestingly, for the climate
723 observed at REN where the number of generations is approximately one, the bark beetle population can only
724 become epidemic t following an intense windthrow event with a 35% damage rate (Fig. 7).
725
726 Throughout the outbreak period, there was a notable decrease in net primary production (*NPP*)(Fig. 7). This decrease
727 is primarily attributed to a sharp decline in leaf area index (not shown). Following the epidemic phase, the leaf area
728 recovers. Following the outbreak: the reduction in stand tree density due to bark beetle damage decreases autotrophic
729 respiration (not shown) and the sparser canopy allows more light to reach the forest floor where it fosters
730 recruitment (not shown), resulting a higher *NPP* or forest growth (Fig. 7). Consequently, carbon use efficiency tends
731 to be higher in sparsely populated stands compared to densely populated ones.
732
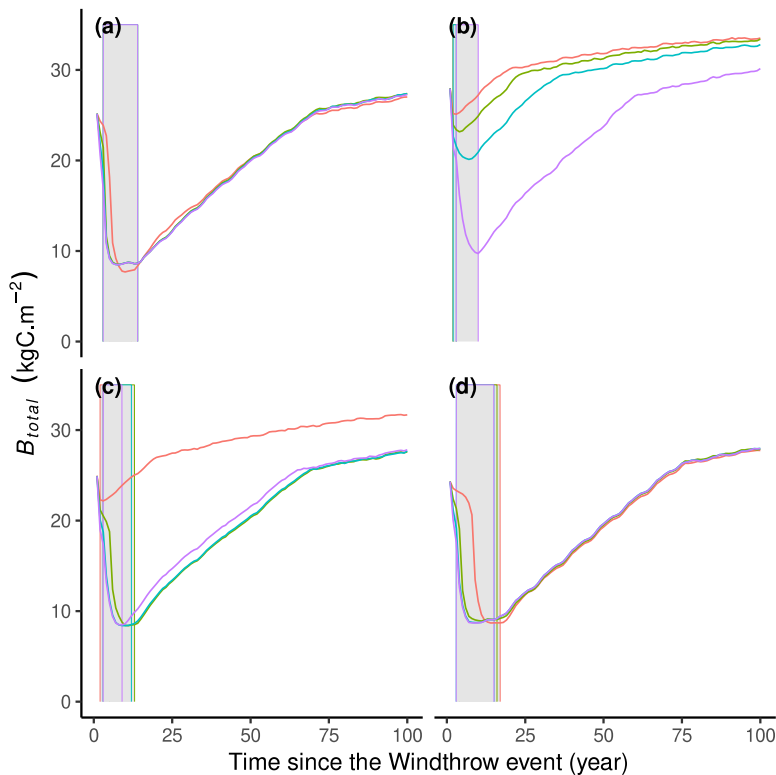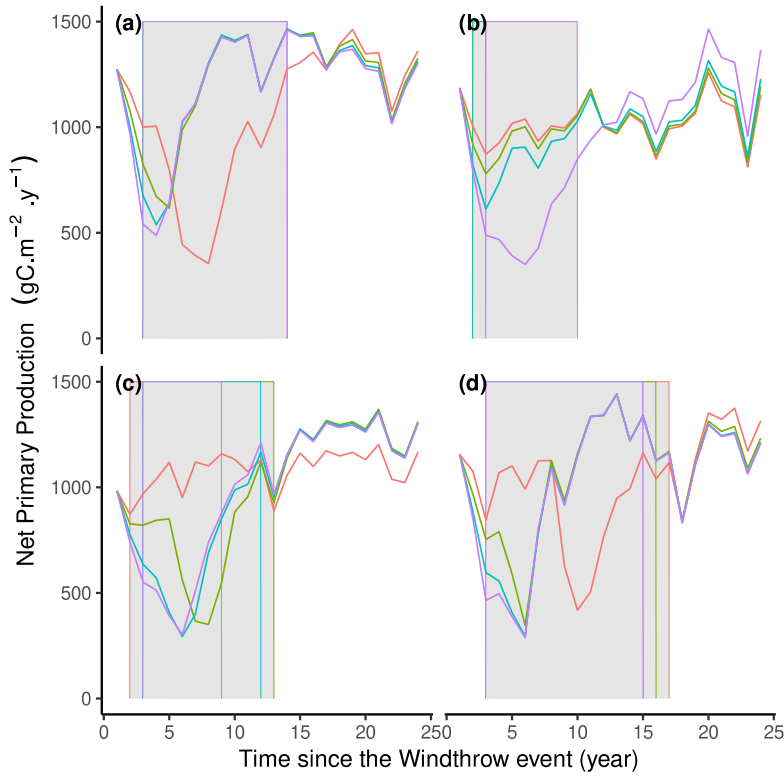
Figure 7: Simulation results of 16 simulations (4 sites x 4 windthrow mortality rate). Lines represent the annual average net primary production (NPP) in gC.m^{-2}.y^{-1} or total stand biomass (B_{total}) in kgC.m^{-2}. *Nbgen* is the average number of bark beetle generations during the five years after the windthrow event. *DR$_{windthrow}$* represents the percentage of biomass loss by a windthrow event at the start of the simulation. Grey areas represent the epidemic phase.

733

734   **4.5. Continuous vs. abrupt mortality**

735
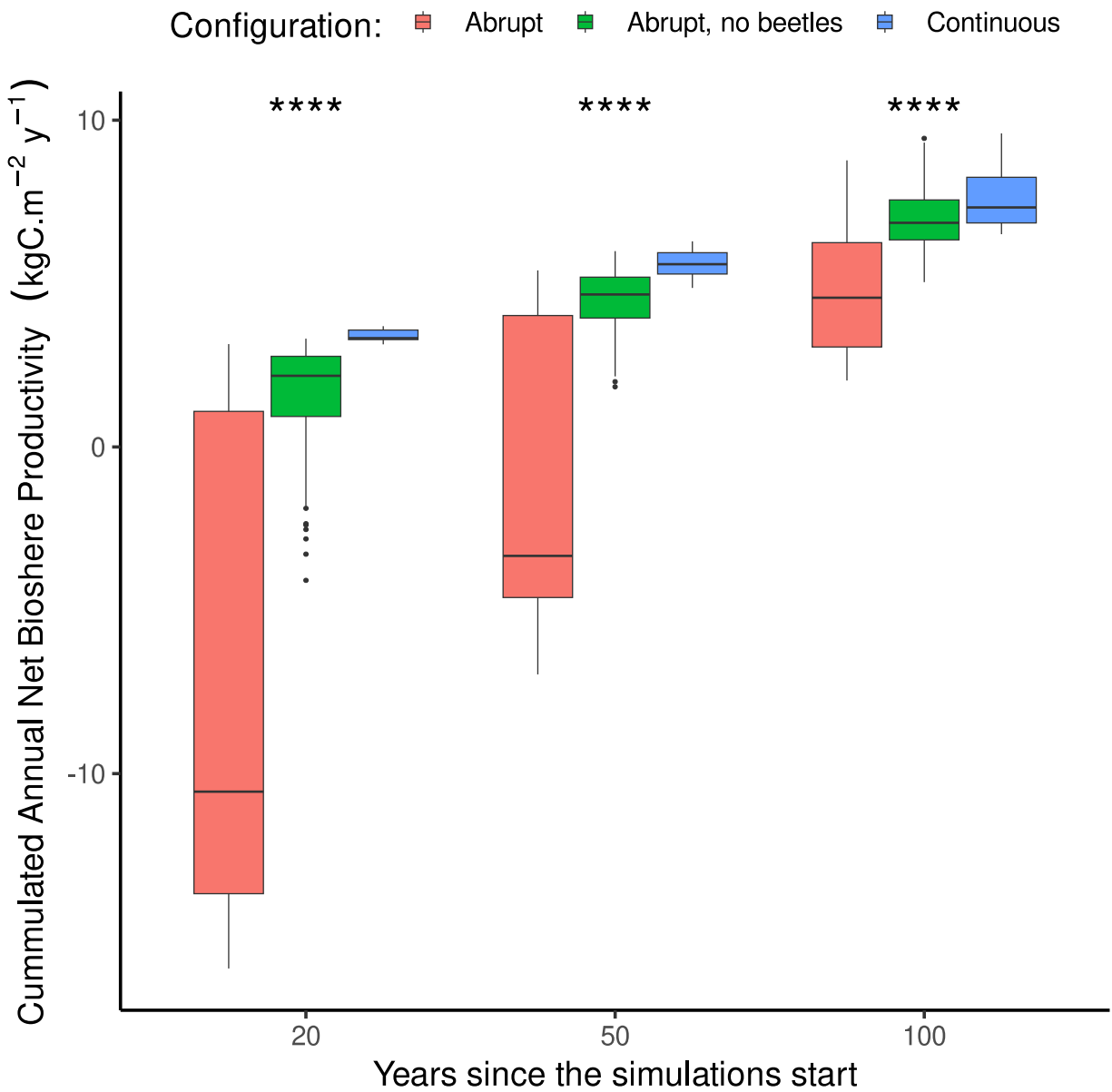
Figure 8: **Difference in cumulative net biome production at three discrete time horizons (i.e. 20, 50 and 100 years) between a fixed continuous mortality rate (blue, n=8), abrupt tree mortality from a windstorm and the subsequent bark beetle outbreak (red, n=56), abrupt mortality from a windstorm not followed by a bark beetles outbreak (green, n=56). Note that in the continuous mortality configuration the mortality rate was adjusted to obtain a similar number of trees killed after 100 years as in the abrupt mortality configuration. The variation of each boxplot arises due to different locations and prescribed storm intensities. Each boxplot displays the median value (thick horizontal line), the quartile range (box border), and the 95% confidence interval (vertical line). A Wilcoxon test between the three configurations at each time horizon showed significant differences (p-value<0001) denoted by the four stars.**

736 The total accumulated net biome production (*NBP*) was evaluated using the ORCHIDEE model across three

737 different timeframes: 20, 50, and 100 years. At the 20-years mark, the average accumulated *NBP* notably differed
738 between the 'continuous', 'abrupt' and the abrupt without bark beetles outbreak ('no beetles') mortality
739 configurations: -7.12±0.97, -1.37±0.28 and 3.39±0.74 kgC.m^{-2}.y^{-1} for the 'abrupt', 'no beetles' and 'continuous'
740 mortality configurations, respectively. These differences were statistically significant (Wilcoxon, p-value<0001),
741 indicating a substantial initial reduction in *NBP* with the 'abrupt' configurations, as ecosystems behaved as carbon
742 sources, whereas under the 'continuous' configuration, they acted as carbon sinks (Fig. 8). The variability in *NBP*
743 demonstrated the broad temperature gradient in Europe and indicated that despite many locations potentially acting
744 as sources under the 'abrupt' configuration, some may transition to carbon sinks within the first 20 years following a
745 disturbance.
746
747 Moving to the 50-years horizon, the difference between the three frameworks decreased, with net biome productions
748 of -0.81±0.60, 4.43±0.15 and 5.61±0.18 kgC.m^{-2}.y^{-1} for the 'abrupt', 'no beetles' and 'continuous' mortality
749 configuration, respectively. The difference in sink strength remained statistically significant (Wilcoxon, p-
750 value<0.001), with the *NBP* in the 'abrupt' configuration approaching carbon neutrality while without the
751 consecutive bark beetles outbreak the ecosystems already became a carbon sink. The climate conditions had a lasting
752 effect on the responses, with the 'abrupt' configuration showing a greater range in responses compared to the
753 'continuous' one.
754
755 At the 100-years mark, the average cumulative *NBP* for the 'abrupts' and 'continuous' configurations approached
756 each other with values of 4.85±0.26, 7.09±0.17 and 7.73±0.40 kgC.m^{-2}.y^{-1}, respectively (Fig. 8) but were still
757 significantly different (Wilcoxon, p-value<0.001). ORCHIDEE simulated a return to a carbon sink (indicated by
758 positive cumulative *NBP* values) suggesting a long-term recovery and potential return to pre-disturbance
759 productivity levels within a century following the windthrow and beetle outbreak event. The 'continuous'
760 configuration displayed a consistently higher median value, suggesting weaker impact of tree mortality dynamics on
761 the long term carbon cycle.
762
763 **5. Discussion**
764   **5.1. Simulating the dynamics of bark beetle outbreaks and their interaction with windthrow**
765 Our *Ips typographus* outbreak model has demonstrated its capability to simulate a broad range of disturbance
766 dynamics. The variation in the outbreak dynamics and the response of the outbreak to its main drivers (Fig. 5 & 6)
767 give confidence in the ability of ORCHIDEE to simulate various outbreak scenarios observed across the temperate
768 and boreal zones under changing climate conditions.
769
770 Windthrow events have significant ecological impact because such disturbances offer fresh breeding substrates,
771 which in turn increase bark beetle populations (Lausch et al., 2011). Our model results align with these findings,
772 indicating that windthrows causing damage of 5% or more may trigger beetle outbreaks (Fig. 6). Additionally, a
773 strong increase in bark beetle populations has been observed following a windthrow event (Wermelinger, 2004), a

774 pattern reflected in the ORCHIDEE simulations. The model simulates a buildup stage spanning 1 to 9 years, where

775 bark beetle numbers increase prior to peaking, with the duration influenced by the severity of the windthrow and the

776 prevailing climate (Fig. 6).

777

778 Temperature is another critical factor affecting bark beetle life cycles. Intra- and interannual variation in temperature

779 impact bark beetles, with warmer conditions fostering multiple generations per year, whereas cooler, damp climates

780 slow breeding and survival rates (Benz et al., 2005). In line with these findings, the temperature dependence of the

781 ORCHIDEE simulations show that cold winters at locations such as SOR and REN reduced bark beetle activity

782 compared to warmer locations like THA and WET (Fig. 6). Lieutier et al. (2004) documented that if the population

783 is large enough, bark beetles can mass attack healthy trees. Our model incorporates this dynamic, illustrated by

784 epidemic stages where living trees become viable hosts, which then exacerbates the growth of the beetle population

785 (Fig. 1).

786

787 The aftermath of a windthrow and subsequent bark beetle outbreak also affects the forest carbon and nitrogen cycles.

788 This impact is observed in the form of snags which are standing dead trees that undergo decomposition. Snags can

789 temporarily disrupt the link between soil and ecosystem carbon and nitrogen dynamics (Rhoades, 2019; Custer et al.,

790 2020). While in ORCHIDEE, the decay of fallen logs does not account for snags yet, the model suggests a recovery

791 period ranging from 5 to 15 years, contingent upon the intensity of the bark beetle outbreak (Fig. 7). As snags create

792 gaps in the canopy, conditions favorable to natural forest regeneration emerge (Jonášová and Prach, 2004) .

793

794 **5.2.**   **Emerging properties from interacting disturbances**

795 While this study did not precisely quantified the impact of simulating abrupt mortality rather than approaching

796 mortality as a continuous process, it demonstrated that the impact of abrupt mortality varies across location and time,

797 i.e. ecosystem functions, such as carbon storage, are affected by natural disturbances like *Ips typographus* outbreaks,

798 having significant impacts on short to mid-term carbon balance estimates (Fig. 8). The simulation experiments also

799 highlighted that the legacy effects of disturbances can endure for decades; even for a simplified representation of

800 forest ecosystems such as ORCHIDEE, where the recovery might be too fast due to the absence of snags (Senf et al.,

801 2017).

802

803 The ability to simulate resistance (i.e., staying essentially unchanged despite the presence of disturbances; Grimm

804 and Wissel, 1997) as an emerging property is evident from Figs. 6 and 7 for locations REN, where no bark beetle

805 outbreaks were observed following a medium windthrow event (5%-20%). However, in all simulated locations that

806 could not resist a bark beetle outbreak, the forest was resilient (i.e., returning to the reference state or dynamic after a

807 temporary disturbance; Grimm and Wissel, 1997) and ecosystem functions were restored to the level from before the

808 windthrow. The elasticity (the speed of return to the reference state or dynamic after a temporary disturbance;

809 Grimm and Wissel, 1997) of the carbon sink capacity ranged from 7 to 14 years. This elasticity is in line with the

810 little observational evidence of ecosystem shifts due to natural disturbances in forests (Millar and Stephenson, 2015).

811 Finally, after the disturbance and the recovery of vegetation structure, the ecosystems simulated by ORCHIDEE
812 showed persistence (i.e. continue along their initial developmental path; Grimm and Wissel, 1997).
813

814   **5.3.**   **Are cascading disturbances important for carbon balance estimates ?**
815 The enhanced complexity introduced into the ORCHIDEE model by incorporating abrupt mortality events, as
816 opposed to a continuous mortality, prompts the question: does this model refinement yield new insights into carbon
817 balance estimates? Our century-long analysis demonstrated that the net biome production, a the metric for carbon
818 sequestration, ultimately converges between the continuous and abrupt mortality frameworks (Fig. 8). This suggests
819 that irrespective of the nature of the mortality events, the forest ecosystem goes through a recovery phase, marked by
820 increased growth that compensates for the growth deficits during the disturbance.
821

822 Yet, our experiment has not taken into account the frequency of disturbances. Given the profound influence of
823 disturbance legacies on carbon dynamics, a recurrence interval shorter than the recovery time of the forest might
824 result in a tipping point. Such a scenario could diminish the carbon sequestration potential of the forest beyond 100-
825 year timeframe, and in extreme cases, may even lead to ecosystem collapse, outcomes not explored in the current
826 simulations nor documented in the recent literature (Millar and Stephenson, 2015).
827

828 In the mid-term, spanning 20 to 50 years, the widely used continuous mortality model appears to inflate the carbon
829 sink capabilities of forests when juxtaposed with abrupt mortality scenarios. Since policy frameworks, including the
830 Green Deal for Europe (2023) and the Paris Agreement |(UNFCCC, 2023), upon these medium-term predictions,
831 they would benefit from adopting model simulations that integrate abrupt mortality events to avoid an
832 overestimation of carbon sink capacities of forest. Furthermore, the accuracy of carbon balance estimates strongly
833 depends upon the initial state of the forest in the model. Forest conditions markedly affect carbon uptake rates. Thus,
834 incorporating an abrupt mortality framework into the ORCHIDEE model could substantially refine and strengthen
835 the predictive power of our carbon balance assessments across short, medium, and long-term scales.
836

837   **5.4.**   **Shortcomings of the bark beetle outbreak model**
838 The bark beetle outbreak model developed in this study builds upon the strengths of the previously established
839 LandClim model, though it also inherited some of its limitations. One notable shortcoming is the model for bark
840 beetle phenology, which is an empirical model making use of accumulated degrees-days. Since the conception of the
841 phenology model a decade ago, Europe's climate has undergone substantial changes, primarily manifested in warmer
842 winters and springs (Copernicus, 2024). Because of these changes, chances have increased for two or even more
843 bark beetle generations within a calendar year (Hlásny et al., 2021a). These changes call for an update of the beetle's
844 phenology model to align with these more recent observations (Ogris et al., 2019).
845

846 A second limitation is that our study, ORCHIDEE, has been parameterized to simulate only *Ips typographus* in
847 Europe. In order to change the beetles and tree host interactions e.g. pine bark beetle in North America

848 (*Dendroctonus monticolae Hopkins*), the sensitivity of indexes must be revised, for example, pine beetle is not

849 breeding on the dead wood falling from withrow but very sensitive to drought events (Preisler et al., 2012). $i_{hosts\,defense}$,

850 and $i_{hosts\,dead}$ as well as the phenology model will need to be revised.

851

852 Another issue is the model's consideration of drought. As outlined in the method section, drought is treated as an

853 exacerbating factor, rather than a primary trigger as is the case for windthrow. This understanding was accurate for

854 *Ips typographus* a decade ago (Temperli et al., 2013); however, emerging evidence increasingly suggests that

855 drought events may indeed trigger bark beetle outbreaks across Europe (Nardi et al., 2023; Netherer et al., 2015).

856 Consequently, this extreme drought as a trigger should be incorporated in a future revision of ORCHIDEE's *Ips*

857 *typographus* outbreak model.

858

859 **6. Outlook**

860 This study simulated the one-way interaction between windthrow and *Ips typographus* outbreaks in unmanaged

861 forests. Future research will incorporate additional interactions, such as: the interplay between droughts, storms, and

862 bark beetles; storms, bark beetles, and fires; as well as forest management, storms, and bark beetles.

863

864 The bark beetle outbreak model could also be enhanced by simulating: (a) standing dead trees (or snags), which

865 would help account for differences in wood decomposition between snags and logs (Angers et al., 2012; Storaunet et

866 al., 2005), (b) the migration of bark beetles to neighboring locations, which becomes significant to account for in a

867 model that operates at spatial resolutions below approximately 10 kilometers, and (c) an up-to-date beetle phenology

868 model which accounts for the recent change in their behavior induced by climate change.

869

870 This research provided an initial qualitative assessment of a new model feature. However, the application of the

871 model necessitates an evaluation of the simulations against observations of cascading disturbances at the regional

872 scale, which is the topic of an ongoing study.

873

874 **7. Conclusion**

875 Our approach enables improving the realism of the *Ips typographus* model in ORCHIDEE without reducing its

876 generality (Levins, 1966). The integration of a bark beetle outbreak model in interaction with other natural

877 disturbance such as windthrow into the ORCHIDEE land surface model has resulted in a broader range of

878 disturbance dynamics and has demonstrated the importance to simulate various disturbance interaction scenarios

879 under different climatic conditions. Incorporating abrupt mortality events instead of a fixed continuous mortality

880 calculation provided new insights into carbon balance estimates. The study showed that the continuous mortality

881 framework, which is commonly used in the land-surface modeling community, tends to overestimate the carbon sink

882 capacity of forests in the 20 to 50 year range in ecosystems under high disturbance pressure, compared to scenarios

883 with abrupt mortality events.

884

Apart from these advances, the study revealed possible shortcomings in the bark beetle outbreak model including the need to update the beetle's phenology model to reflect recent climate changes, and the need to consider extreme drought as a trigger for bark beetle outbreaks in line with emerging evidence. Looking ahead, future work will further develop the capability of ORCHIDEE to simulate interacting disturbances such as the interplay between extreme droughts, storms, and bark beetles, and between storms, bark beetles, and fires.

The final step will be a quantitative evaluation based on observed data (Marini et al., 2017) in order to assess the capability of ORCHIDEE to simulate complex interaction between multiple sources of tree mortality affecting the carbon balance at large scale.

8. Code availability

- R script and data are available at :
    https://doi.org/10.5281/zenodo.12806280
- ORCHIDEE rev 7791 code is also available from:
    https://forge.ipsl.jussieu.fr/orchidee/browser/branches/publications/
ORCHIDEE_Bark_beetles_outbreak_gmd_2024

9. Data availability

- The Fluxnet climate forcing data are available at https://fluxnet.org/
- The simulation results use in this study are available at https://doi.org/10.5281/zenodo.12806280

10. Author contribution

G. Marie, S. Luyssaert designed the experiments and G. Marie conducted them. Following discussions with H. Jactel, G. Petter and M. Cailleret, G. Marie developed the bark beetles model code and performed the simulations. J. Jeong integrated the wind damage and bark beetle models with each other. G. Marie, J. Jeong, V. Bastrikov, J. Ghattas, B. Guenet, A.S. Lansø, M.J. McGrath, K. Naudts, A. Valade, C. Yue, and S. Luyssaert, contributed to the development, parameterization and evaluation of the ORCHIDEE revision used in this study. G. Marie, J. Jeong, and S. Luyssaert prepared the manuscript with contributions from all co-authors.

11. Competing interests

No competing interest

12. Acknowledgements

13. References

Abramowitz, G., Leuning, R., Clark, M., and Pitman, A.: Evaluating the Performance of Land Surface Models, J. Clim., 21, 5468–5481, https://doi.org/10.1175/2008JCLI2378.1, 2008.

Allen, C. D., Breshears, D. D., and McDowell, N. G.: On underestimation of global vulnerability to tree mortality and forest die-off from hotter drought in the Anthropocene, Ecosphere, 6, art129, https://doi.org/10.1890/ES15-00203.1, 2015.

Andrus, R. A., Hart, S. J., and Veblen, T. T.: Forest recovery following synchronous outbreaks of spruce and western balsam bark beetle is slowed by ungulate browsing, Ecology, 101, e02998, https://doi.org/10.1002/ecy.2998, 2020.

Angers, V. A., Drapeau, P., and Bergeron, Y.: Mineralization rates and factors influencing snag decay in four North American boreal tree species, Can. J. For. Res., 42, 157–166, https://doi.org/10.1139/x11-167, 2012.

European State of the Climate | Copernicus: https://climate.copernicus.eu/ESOTC, last access: 25 March 2024.

Bakke, A.: The recent Ips typographus outbreak in Norway - experiences from a control program, Ecography, 12, 515–519, https://doi.org/10.1111/j.1600-0587.1989.tb00930.x, 1989.

Ballard, R. G., Walsh, M. A., and Cole, W. E.: Blue-stain fungi in xylem of lodgepole pine: a light-microscope study on extent of hyphal distribution, Can. J. Bot., 60, 2334–2341, https://doi.org/10.1139/b82-285, 1982.

Bentz, B. J., Régnière, J., Fettig, C. J., Hansen, E. M., Hayes, J. L., Hicke, J. A., Kelsey, R. G., Negrón, J. F., and Seybold, S. J.: Climate Change and Bark Beetles of the Western United States and Canada: Direct and Indirect Effects, BioScience, 60, 602–613, https://doi.org/10.1525/bio.2010.60.8.6, 2010.

Berner, L. T., Law, B. E., Meddens, A. J. H., and Hicke, J. A.: Tree mortality from fires, bark beetles, and timber harvest during a hot and dry decade in the western United States (2003–2012), Environ. Res. Lett., 12, 065005, https://doi.org/10.1088/1748-9326/aa6f94, 2017.

Berryman, A. A.: Population Cycles: The Case for Trophic Interactions, Oxford University Press, 207 pp., 2002.

Biedermann, P. H. W., Müller, J., Grégoire, J.-C., Gruppe, A., Hagge, J., Hammerbacher, A., Hofstetter, R. W., Kandasamy, D., Kolarik, M., Kostovcik, M., Krokene, P., Sallé, A., Six, D. L., Turrini, T., Vanderpool, D., Wingfield, M. J., and Bässler, C.: Bark Beetle Population Dynamics in the Anthropocene: Challenges and Solutions, Trends Ecol. Evol., 34, 914–924, https://doi.org/10.1016/j.tree.2019.06.002, 2019.

Boucher, O., Servonnat, J., Albright, A. L., Aumont, O., Balkanski, Y., Bastrikov, V., Bekki, S., Bonnet, R., Bony, S., Bopp, L., Braconnot, P., Brockmann, P., Cadule, P., Caubel, A., Cheruy, F., Codron, F., Cozic, A., Cugnet, D., D'Andrea, F., Davini, P., Lavergne, C. de, Denvil, S., Deshayes, J., Devilliers, M., Ducharne, A., Dufresne, J.-L., Dupont, E., Éthé, C., Fairhead, L., Falletti, L., Flavoni, S., Foujols, M.-A., Gardoll, S., Gastineau, G., Ghattas, J., Grandpeix, J.-Y., Guenet, B., Guez, L., E., Guilyardi, E., Guimberteau, M., Hauglustaine, D., Hourdin, F., Idelkadi, A., Joussaume, S., Kageyama, M., Khodri, M., Krinner, G., Lebas, N., Levavasseur, G., Lévy, C., Li, L., Lott, F., Lurton, T., Luyssaert, S., Madec, G., Madeleine, J.-B., Maignan, F., Marchand, M., Marti, O., Mellul, L., Meurdesoif, Y., Mignot, J., Musat, I., Ottlé, C., Peylin, P., Planton, Y., Polcher, J., Rio, C., Rochetin, N., Rousset, C., Sepulchre, P., Sima, A., Swingedouw, D., Thiéblemont, R., Traore, A. K., Vancoppenolle, M., Vial, J., Vialard, J., Viovy, N., and Vuichard, N.: Presentation and Evaluation of the IPSL-CM6A-LR Climate Model, J. Adv. Model. Earth Syst., 12, e2019MS002010, https://doi.org/10.1029/2019MS002010, 2020.

Bugmann, H. K. M.: A Simplified Forest Model to Study Species Composition Along Climate Gradients, Ecology, 77, 2055–2074, https://doi.org/10.2307/2265700, 1996.

Buma, B.: Disturbance interactions: characterization, prediction, and the potential for cascading effects, Ecosphere, 6, art70, https://doi.org/10.1890/ES15-00058.1, 2015.

Chen, Y., Ryder, J., Bastrikov, V., McGrath, M. J., Naudts, K., Otto, J., Ottlé, C., Peylin, P., Polcher, J., Valade, A.,

973 Black, A., Elbers, J. A., Moors, E., Foken, T., van Gorsel, E., Haverd, V., Heinesch, B., Tiedemann, F., Knohl, A.,
974 Launiainen, S., Loustau, D., Ogée, J., Vessala, T., and Luyssaert, S.: Evaluating the performance of land surface
975 model ORCHIDEE-CAN v1.0 on water and energy flux estimation with a single- and multi-layer energy budget
976 scheme, Geosci. Model Dev., 9, 2951–2972, https://doi.org/10.5194/gmd-9-2951-2016, 2016.
977 Chen, Y.-Y., Gardiner, B., Pasztor, F., Blennow, K., Ryder, J., Valade, A., Naudts, K., Otto, J., McGrath, M. J.,
978 Planque, C., and Luyssaert, S.: Simulating damage for wind storms in the land surface model ORCHIDEE-CAN
979 (revision 4262), Geosci. Model Dev., 11, 771–791, https://doi.org/10.5194/gmd-11-771-2018, 2018.
980 Ciais, P., Reichstein, M., Viovy, N., Granier, A., Ogée, J., Allard, V., Aubinet, M., Buchmann, N., Bernhofer, C.,
981 Carrara, A., Chevallier, F., De Noblet, N., Friend, A. D., Friedlingstein, P., Grünwald, T., Heinesch, B., Keronen, P.,
982 Knohl, A., Krinner, G., Loustau, D., Manca, G., Matteucci, G., Miglietta, F., Ourcival, J. M., Papale, D., Pilegaard,
983 K., Rambal, S., Seufert, G., Soussana, J. F., Sanz, M. J., Schulze, E. D., Vesala, T., and Valentini, R.: Europe-wide
984 reduction in primary productivity caused by the heat and drought in 2003, Nature, 437, 529–533,
985 https://doi.org/10.1038/nature03972, 2005.
986 Cox, P. M., Betts, R. A., Jones, C. D., Spall, S. A., and Totterdell, I. J.: Acceleration of global warming due to
987 carbon-cycle feedbacks in a coupled climate model, Nature, 408, 184–187, https://doi.org/10.1038/35041539, 2000.
988 Custer, G. F., van Diepen, L. T. A., and Stump, W. L.: Structural and Functional Dynamics of Soil Microbes
989 following Spruce Beetle Infestation, Appl. Environ. Microbiol., 86, e01984-19, https://doi.org/10.1128/AEM.01984-
990 19, 2020.
991 Das, A. J., Stephenson, N. L., and Davis, K. P.: Why do trees die? Characterizing the drivers of background tree
992 mortality, Ecology, 97, 2616–2627, https://doi.org/10.1002/ecy.1497, 2016.
993 Deleuze, C., Pain, O., Dhôte, J.-F., and Hervé, J.-C.: A flexible radial increment model for individual trees in pure
994 even-aged stands, Ann. For. Sci., 61, 327–335, https://doi.org/10.1051/forest:2004026, 2004.
995 Edburg, S. L., Hicke, J. A., Brooks, P. D., Pendall, E. G., Ewers, B. E., Norton, U., Gochis, D., Gutmann, E. D., and
996 Meddens, A. J.: Cascading impacts of bark beetle-caused tree mortality on coupled biogeophysical and
997 biogeochemical processes, Front. Ecol. Environ., 10, 416–424, https://doi.org/10.1890/110173, 2012.
998 Faccoli, M. and Stergulc, F.: A practical method for predicting the short-time trend of bivoltine populations of Ips
999 typographus (L.) (Col., Scolytidae), J. Appl. Entomol., 130, 61–66, https://doi.org/10.1111/j.1439-
1000 0418.2005.01019.x, 2006.
1001 Friedlingstein, P., Cox, P., Betts, R., Bopp, L., Bloh, W. von, Brovkin, V., Cadule, P., Doney, S., Eby, M., Fung, I.,
1002 Bala, G., John, J., Jones, C., Joos, F., Kato, T., Kawamiya, M., Knorr, W., Lindsay, K., Matthews, H. D., Raddatz,
1003 T., Rayner, P., Reick, C., Roeckner, E., Schnitzler, K.-G., Schnur, R., Strassmann, K., Weaver, A. J., Yoshikawa, C.,
1004 and Zeng, N.: Climate–Carbon Cycle Feedback Analysis: Results from the C4MIP Model Intercomparison, J. Clim.,
1005 19, 3337–3353, https://doi.org/10.1175/JCLI3800.1, 2006.
1006 Grimm, V. and Wissel, C.: Babel, or the ecological stability discussions: an inventory and analysis of terminology
1007 and a guide for avoiding confusion, Oecologia, 109, 323–334, https://doi.org/10.1007/s004420050090, 1997.
1008 Havašová, M., Ferenčík, J., and Jakuš, R.: Interactions between windthrow, bark beetles and forest management in
1009 the Tatra national parks, For. Ecol. Manag., 391, 349–361, https://doi.org/10.1016/j.foreco.2017.01.009, 2017.
1010 Haverd, V., Lovell, J. L., Cuntz, M., Jupp, D. L. B., Newnham, G. J., and Sea, W.: The Canopy Semi-analytic Pgap
1011 And Radiative Transfer (CanSPART) model: Formulation and application, Agric. For. Meteorol., 160, 14–35,
1012 https://doi.org/10.1016/j.agrformet.2012.01.018, 2012.
1013 Hicke, J. A., Allen, C. D., Desai, A. R., Dietze, M. C., Hall, R. J., Hogg, E. H., Kashian, D. M., Moore, D., Raffa, K.
1014 F., Sturrock, R. N., and Vogelmann, J.: Effects of biotic disturbances on forest carbon cycling in the United States
1015 and Canada., https://doi.org/10.1111/j.1365-2486.2011.02543.x, 2012.
1016 Hlásny, T., König, L., Krokene, P., Lindner, M., Montagné-Huck, C., Müller, J., Qin, H., Raffa, K. F., Schelhaas,
1017 M.-J., Svoboda, M., Viiri, H., and Seidl, R.: Bark Beetle Outbreaks in Europe: State of Knowledge and Ways
1018 Forward for Management, Curr. For. Rep., 7, 138–165, https://doi.org/10.1007/s40725-021-00142-x, 2021a.
1019 Hlásny, T., Zimová, S., Merganičová, K., Štěpánek, P., Modlinger, R., and Turčáni, M.: Devastating outbreak of
1020 bark beetles in the Czech Republic: Drivers, impacts, and management implications, For. Ecol. Manag., 490,
1021 119075, https://doi.org/10.1016/j.foreco.2021.119075, 2021b.
1022 Huang, J., Kautz, M., Trowbridge, A. M., Hammerbacher, A., Raffa, K. F., Adams, H. D., Goodsman, D. W., Xu,
1023 C., Meddens, A. J. H., Kandasamy, D., Gershenzon, J., Seidl, R., and Hartmann, H.: Tree defence and bark beetles in
1024 a drying world: carbon partitioning, functioning and modelling, New Phytol., 225, 26–36,
1025 https://doi.org/10.1111/nph.16173, 2020.
1026 Jönsson, A. M., Appelberg, G., Harding, S., and Bärring, L.: Spatio-temporal impact of climate change on the
1027 activity and voltinism of the spruce bark beetle, Ips typographus, Glob. Change Biol., 15, 486–499,
1028 https://doi.org/10.1111/j.1365-2486.2008.01742.x, 2009.

Jönsson, A. M., Harding, S., Krokene, P., Lange, H., Lindelöw, Å., Økland, B., Ravn, H. P., and Schroeder, L. M.: Modelling the potential impact of global warming on Ips typographus voltinism and reproductive diapause, Clim. Change, 109, 695–718, https://doi.org/10.1007/s10584-011-0038-4, 2011.

Jönsson, A. M., Schroeder, L. M., Lagergren, F., Anderbrant, O., and Smith, B.: Guess the impact of *Ips typographus*—An ecosystem modelling approach for simulating spruce bark beetle outbreaks, Agric. For. Meteorol., 166–167, 188–200, https://doi.org/10.1016/j.agrformet.2012.07.012, 2012.

Kärvemo, S. and Schroeder, L. M.: A comparison of outbreak dynamics of the spruce bark beetle in Sweden and the mountain pine beetle in Canada (Curculionidae: Scolytinae), 2010.

Kautz, M., Anthoni, P., Meddens, A. J. H., Pugh, T. A. M., and Arneth, A.: Simulating the recent impacts of multiple biotic disturbances on forest carbon cycling across the United States, Glob. Change Biol., 24, 2079–2092, https://doi.org/10.1111/gcb.13974, 2018.

Komonen, A., Schroeder, L. M., and Weslien, J.: Ips typographus population development after a severe storm in a nature reserve in southern Sweden, J. Appl. Entomol., 135, 132–141, https://doi.org/10.1111/j.1439-0418.2010.01520.x, 2011.

Krinner, G., Viovy, N., de Noblet-Ducoudré, N., Ogée, J., Polcher, J., Friedlingstein, P., Ciais, P., Sitch, S., and Prentice, I. C.: A dynamic global vegetation model for studies of the coupled atmosphere-biosphere system: DVGM FOR COUPLED CLIMATE STUDIES, Glob. Biogeochem. Cycles, 19, https://doi.org/10.1029/2003GB002199, 2005.

Kurz, W. A., Dymond, C. C., Stinson, G., Rampley, G. J., Neilson, E. T., Carroll, A. L., Ebata, T., and Safranyik, L.: Mountain pine beetle and forest carbon feedback to climate change, Nature, 452, 987–990, https://doi.org/10.1038/nature06777, 2008a.

Kurz, W. A., Dymond, C. C., Stinson, G., Rampley, G. J., Neilson, E. T., Carroll, A. L., Ebata, T., and Safranyik, L.: Mountain pine beetle and forest carbon feedback to climate change, Nature, 452, 987–990, https://doi.org/10.1038/nature06777, 2008b.

Kurz, W. A., Stinson, G., Rampley, G. J., Dymond, C. C., and Neilson, E. T.: Risk of natural disturbances makes future contribution of Canada's forests to the global carbon cycle highly uncertain, Proc. Natl. Acad. Sci., 105, 1551–1555, https://doi.org/10.1073/pnas.0708133105, 2008c.

Lasslop, G., Thonicke, K., and Kloster, S.: SPITFIRE within the MPI Earth system model: Model development and evaluation, J. Adv. Model. Earth Syst., 6, 740–755, https://doi.org/10.1002/2013MS000284, 2014.

Lausch, A., Fahse, L., and Heurich, M.: Factors affecting the spatio-temporal dispersion of *Ips typographus* (L.) in Bavarian Forest National Park: A long-term quantitative landscape-level analysis, For. Ecol. Manag., 261, 233–245, https://doi.org/10.1016/j.foreco.2010.10.012, 2011.

Levins, R.: The Strategy of Model Building in Population Biology, Am. Sci., 54, 421–431, 1966.

Lieutier, F.: Mechanisms of Resistance in Conifers and Bark beetle Attack Strategies, in: Mechanisms and Deployment of Resistance in Trees to Insects, edited by: Wagner, M. R., Clancy, K. M., Lieutier, F., and Paine, T. D., Springer Netherlands, Dordrecht, 31–77, https://doi.org/10.1007/0-306-47596-0_2, 2002.

Lombardero, M. J., Ayres, M. P., Ayres, B. D., and Reeve, J. D.: Cold Tolerance of Four Species of Bark Beetle (Coleoptera: Scolytidae) in North America, Environ. Entomol., 29, 421–432, https://doi.org/10.1603/0046-225X-29.3.421, 2000.

Luyssaert, S., Marie, G., Valade, A., Chen, Y.-Y., Njakou Djomo, S., Ryder, J., Otto, J., Naudts, K., Lansø, A. S., Ghattas, J., and McGrath, M. J.: Trade-offs in using European forests to meet climate objectives, Nature, 562, 259–262, https://doi.org/10.1038/s41586-018-0577-1, 2018.

Marini, L., Økland, B., Jönsson, A. M., Bentz, B., Carroll, A., Forster, B., Grégoire, J.-C., Hurling, R., Nageleisen, L. M., Netherer, S., Ravn, H. P., Weed, A., and Schroeder, M.: Climate drivers of bark beetle outbreak dynamics in Norway spruce forests, Ecography, 40, 1426–1435, https://doi.org/10.1111/ecog.02769, 2017.

Mezei, P., Grodzki, W., Blaženec, M., and Jakuš, R.: Factors influencing the *wind–bark beetles'* disturbance system in the course of an *Ips typographus* outbreak in the Tatra Mountains, For. Ecol. Manag., 312, 67–77, https://doi.org/10.1016/j.foreco.2013.10.020, 2014.

Mezei, P., Jakuš, R., Pennerstorfer, J., Havašová, M., Škvarenina, J., Ferenčík, J., Slivinský, J., Bičárová, S., Bilčík, D., Blaženec, M., and Netherer, S.: Storms, temperature maxima and the Eurasian spruce bark beetle *Ips typographus*—An infernal trio in Norway spruce forests of the Central European High Tatra Mountains, Agric. For. Meteorol., 242, 85–95, https://doi.org/10.1016/j.agrformet.2017.04.004, 2017.

Migliavacca, M., Dosio, A., Kloster, S., Ward, D. S., Camia, A., Houborg, R., Houston Durrant, T., Khabarov, N., Krasovskii, A. A., San Miguel-Ayanz, J., and Cescatti, A.: Modeling burned area in Europe with the Community Land Model, J. Geophys. Res. Biogeosciences, 118, 265–279, https://doi.org/10.1002/jgrg.20026, 2013.

Migliavacca, M., Musavi, T., Mahecha, M. D., Nelson, J. A., Knauer, J., Baldocchi, D. D., Perez-Priego, O.,

Christiansen, R., Peters, J., Anderson, K., Bahn, M., Black, T. A., Blanken, P. D., Bonal, D., Buchmann, N., Caldararu, S., Carrara, A., Carvalhais, N., Cescatti, A., Chen, J., Cleverly, J., Cremonese, E., Desai, A. R., El-Madany, T. S., Farella, M. M., Fernández-Martínez, M., Filippa, G., Forkel, M., Galvagno, M., Gomarasca, U., Gough, C. M., Göckede, M., Ibrom, A., Ikawa, H., Janssens, I. A., Jung, M., Kattge, J., Keenan, T. F., Knohl, A., Kobayashi, H., Kraemer, G., Law, B. E., Liddell, M. J., Ma, X., Mammarella, I., Martini, D., Macfarlane, C., Matteucci, G., Montagnani, L., Pabon-Moreno, D. E., Panigada, C., Papale, D., Pendall, E., Penuelas, J., Phillips, R. P., Reich, P. B., Rossini, M., Rotenberg, E., Scott, R. L., Stahl, C., Weber, U., Wohlfahrt, G., Wolf, S., Wright, I. J., Yakir, D., Zaehle, S., and Reichstein, M.: The three major axes of terrestrial ecosystem function, Nature, 598, 468–472, https://doi.org/10.1038/s41586-021-03939-9, 2021.

Millar, C. I. and Stephenson, N. L.: Temperate forest health in an era of emerging megadisturbance, Science, 349, 823–826, https://doi.org/10.1126/science.aaa9933, 2015.

Morehouse, K., Johns, T., Kaye, J., and Kaye, M.: Carbon and nitrogen cycling immediately following bark beetle outbreaks in southwestern ponderosa pine forests, For. Ecol. Manag., 255, 2698–2708, https://doi.org/10.1016/j.foreco.2008.01.050, 2008.

Nardi, D., Jactel, H., Pagot, E., Samalens, J.-C., and Marini, L.: Drought and stand susceptibility to attacks by the European spruce bark beetle: A remote sensing approach, Agric. For. Entomol., 25, 119–129, https://doi.org/10.1111/afe.12536, 2023.

Naudts, K., Ryder, J., McGrath, M. J., Otto, J., Chen, Y., Valade, A., Bellasen, V., Berhongaray, G., Bönisch, G., Campioli, M., and others: A vertically discretised canopy description for ORCHIDEE (SVN r2290) and the modifications to the energy, water and carbon fluxes, Geosci. Model Dev., 8, 2035–2065, 2015a.

Naudts, K., Ryder, J., McGrath, M. J., Otto, J., Chen, Y., Valade, A., Bellasen, V., Berhongaray, G., Bönisch, G., Campioli, M., Ghattas, J., De Groote, T., Haverd, V., Kattge, J., MacBean, N., Maignan, F., Merilä, P., Penuelas, J., Peylin, P., Pinty, B., Pretzsch, H., Schulze, E. D., Solyga, D., Vuichard, N., Yan, Y., and Luyssaert, S.: A vertically discretised canopy description for ORCHIDEE (SVN r2290) and the modifications to the energy, water and carbon fluxes, Geosci. Model Dev., 8, 2035–2065, https://doi.org/10.5194/gmd-8-2035-2015, 2015b.

Naudts, K., Chen, Y., McGrath, M. J., Ryder, J., Valade, A., Otto, J., and Luyssaert, S.: Europe's forest management did not mitigate climate warming, Science, 351, 597–600, https://doi.org/10.1126/science.aad7270, 2016.

Netherer, S., Matthews, B., Katzensteiner, K., Blackwell, E., Henschke, P., Hietz, P., Pennerstorfer, J., Rosner, S., Kikuta, S., Schume, H., and Schopf, A.: Do water-limiting conditions predispose Norway spruce to bark beetle attack?, New Phytol., 205, 1128–1141, https://doi.org/10.1111/nph.13166, 2015.

Ogris, N., Ferlan, M., Hauptman, T., Pavlin, R., Kavčič, A., Jurc, M., and de Groot, M.: RITY – A phenology model of *Ips typographus* as a tool for optimization of its monitoring, Ecol. Model., 410, 108775, https://doi.org/10.1016/j.ecolmodel.2019.108775, 2019.

Pastorello, G., Trotta, C., Canfora, E., Chu, H., Christianson, D., Cheah, Y.-W., Poindexter, C., Chen, J., Elbashandy, A., Humphrey, M., Isaac, P., Polidori, D., Reichstein, M., Ribeca, A., van Ingen, C., Vuichard, N., Zhang, L., Amiro, B., Ammann, C., Arain, M. A., Ardö, J., Arkebauer, T., Arndt, S. K., Arriga, N., Aubinet, M., Aurela, M., Baldocchi, D., Barr, A., Beamesderfer, E., Marchesini, L. B., Bergeron, O., Beringer, J., Bernhofer, C., Berveiller, D., Billesbach, D., Black, T. A., Blanken, P. D., Bohrer, G., Boike, J., Bolstad, P. V., Bonal, D., Bonnefond, J.-M., Bowling, D. R., Bracho, R., Brodeur, J., Brümmer, C., Buchmann, N., Burban, B., Burns, S. P., Buysse, P., Cale, P., Cavagna, M., Cellier, P., Chen, S., Chini, I., Christensen, T. R., Cleverly, J., Collalti, A., Consalvo, C., Cook, B. D., Cook, D., Coursolle, C., Cremonese, E., Curtis, P. S., D'Andrea, E., da Rocha, H., Dai, X., Davis, K. J., Cinti, B. D., Grandcourt, A. de, Ligne, A. D., De Oliveira, R. C., Delpierre, N., Desai, A. R., Di Bella, C. M., Tommasi, P. di, Dolman, H., Domingo, F., Dong, G., Dore, S., Duce, P., Dufrêne, E., Dunn, A., Dušek, J., Eamus, D., Eichelmann, U., ElKhidir, H. A. M., Eugster, W., Ewenz, C. M., Ewers, B., Famulari, D., Fares, S., Feigenwinter, I., Feitz, A., Fensholt, R., Filippa, G., Fischer, M., Frank, J., Galvagno, M., et al.: The FLUXNET2015 dataset and the ONEFlux processing pipeline for eddy covariance data, Sci. Data, 7, 225, https://doi.org/10.1038/s41597-020-0534-3, 2020.

Pasztor, F., Matulla, C., Rammer, W., and Lexer, M. J.: Drivers of the bark beetle disturbance regime in Alpine forests in Austria, For. Ecol. Manag., 318, 349–358, https://doi.org/10.1016/j.foreco.2014.01.044, 2014.

Pfeifer, E. M., Hicke, J. A., and Meddens, A. J. H.: Observations and modeling of aboveground tree carbon stocks and fluxes following a bark beetle outbreak in the western United States, Glob. Change Biol., 17, 339–350, https://doi.org/10.1111/j.1365-2486.2010.02226.x, 2011.

Pineau, X., David, G., Peter, Z., Sallé, A., Baude, M., Lieutier, F., and Jactel, H.: Effect of temperature on the reproductive success, developmental rate and brood characteristics of Ips sexdentatus (Boern.), Agric. For. Entomol., 19, 23–33, https://doi.org/10.1111/afe.12177, 2017.

Preisler, H. K., Hicke, J. A., Ager, A. A., and Hayes, J. L.: Climate and weather influences on spatial temporal

patterns of mountain pine beetle populations in Washington and Oregon, Ecology, 93, 2421–2434, https://doi.org/10.1890/11-1412.1, 2012.

Pugh, T. A. M., Jones, C. D., Huntingford, C., Burton, C., Arneth, A., Brovkin, V., Ciais, P., Lomas, M., Robertson, E., and Piao, S. L.: A Large Committed Long-Term Sink of Carbon due to Vegetation Dynamics, Earths Future, 2017.

Quillet, A., Peng, C., and Garneau, M.: Toward dynamic global vegetation models for simulating vegetation–climate interactions and feedbacks: recent developments, limitations, and future challenges, Environ. Rev., 18, 333–353, https://doi.org/10.1139/A10-016, 2010.

Raffa, K. F., Aukema, B. H., Bentz, B. J., Carroll, A. L., Hicke, J. A., Turner, M. G., and Romme, W. H.: Cross-scale Drivers of Natural Disturbances Prone to Anthropogenic Amplification: The Dynamics of Bark Beetle Eruptions, BioScience, 58, 501–517, https://doi.org/10.1641/B580607, 2008.

Ryder, J., Polcher, J., Peylin, P., Ottlé, C., Chen, Y., van Gorsel, E., Haverd, V., McGrath, M. J., Naudts, K., Otto, J., Valade, A., and Luyssaert, S.: A multi-layer land surface energy budget model for implicit coupling with global atmospheric simulations, Geosci. Model Dev., 9, 223–245, https://doi.org/10.5194/gmd-9-223-2016, 2016.

Schumacher, S.: The role of large-scale disturbances and climate for the dynamics of forested landscapes in the European Alps, Doctoral Thesis, ETH Zurich, https://doi.org/10.3929/ethz-a-004818825, 2004.

Seidl, R. and Rammer, W.: Climate change amplifies the interactions between wind and bark beetle disturbances in forest landscapes, Landsc. Ecol., 1–14, https://doi.org/10.1007/s10980-016-0396-4, 2016.

Seidl, R., Fernandes, P. M., Fonseca, T. F., Gillet, F., Jönsson, A. M., Merganičová, K., Netherer, S., Arpaci, A., Bontemps, J.-D., Bugmann, H., González-Olabarria, J. R., Lasch, P., Meredieu, C., Moreira, F., Schelhaas, M.-J., and Mohren, F.: Modelling natural disturbances in forest ecosystems: a review, Ecol. Model., 222, 903–924, https://doi.org/10.1016/j.ecolmodel.2010.09.040, 2011.

Seidl, R., Schelhaas, M.-J., Rammer, W., and Verkerk, P. J.: Increasing forest disturbances in Europe and their impact on carbon storage, Nat. Clim. Change, 4, 806–810, https://doi.org/10.1038/nclimate2318, 2014.

Seidl, R., Thom, D., Kautz, M., Martin-Benito, D., Peltoniemi, M., Vacchiano, G., Wild, J., Ascoli, D., Petr, M., Honkaniemi, J., Lexer, M. J., Trotsiuk, V., Mairota, P., Svoboda, M., Fabrika, M., Nagel, T. A., and Reyer, C. P. O.: Forest disturbances under climate change, Nat. Clim. Change, 7, 395–402, https://doi.org/10.1038/nclimate3303, 2017.

Seidl, R., Klonner, G., Rammer, W., Essl, F., Moreno, A., Neumann, M., and Dullinger, S.: Invasive alien pests threaten the carbon stored in Europe's forests, Nat. Commun., 9, 1626, https://doi.org/10.1038/s41467-018-04096-w, 2018.

Senf, C., Pflugmacher, D., Hostert, P., and Seidl, R.: Using Landsat time series for characterizing forest disturbance dynamics in the coupled human and natural systems of Central Europe, ISPRS J. Photogramm. Remote Sens., 130, 453–463, https://doi.org/10.1016/j.isprsjprs.2017.07.004, 2017.

Storaunet, K. O., Rolstad, J., Gjerde, I., and Gundersen, V. S.: Historical logging, productivity, and structural characteristics of boreal coniferous forests in Norway, Silva Fenn., 39, 2005.

Temperli, C., Bugmann, H., and Elkin, C.: Cross-scale interactions among bark beetles, climate change, and wind disturbances: a landscape modeling approach, Ecol. Monogr., 83, 383–402, https://doi.org/10.1890/12-1503.1, 2013a.

Temperli, C., Bugmann, H., and Elkin, C.: Cross-scale interactions among bark beetles, climate change, and wind disturbances: a landscape modeling approach, Ecol. Monogr., 83, 383–402, https://doi.org/10.1890/12-1503.1, 2013b.

Thurner, M., Beer, C., Ciais, P., Friend, A. D., Ito, A., Kleidon, A., Lomas, M. R., Quegan, S., Rademacher, T. T., Schaphoff, S., Tum, M., Wiltshire, A., and Carvalhais, N.: Evaluation of climate-related carbon turnover processes in global vegetation models for boreal and temperate forests, Glob. Change Biol., 23, 3076–3091, https://doi.org/10.1111/gcb.13660, 2017.

Van Meerbeek, K., Jucker, T., and Svenning, J.-C.: Unifying the concepts of stability and resilience in ecology, J. Ecol., 109, 3114–3132, https://doi.org/10.1111/1365-2745.13651, 2021.

Vuichard, N., Messina, P., Luyssaert, S., Guenet, B., Zaehle, S., Ghattas, J., Bastrikov, V., and Peylin, P.: Accounting for carbon and nitrogen interactions in the global terrestrial ecosystem model ORCHIDEE (trunk version, rev 4999): multi-scale evaluation of gross primary production, Geosci. Model Dev., 12, 4751–4779, https://doi.org/10.5194/gmd-12-4751-2019, 2019.

Wermelinger, B.: Ecology and management of the spruce bark beetle Ips typographus—a review of recent research, For. Ecol. Manag., 202, 67–82, https://doi.org/10.1016/j.foreco.2004.07.018, 2004.

Wichmann, L. and Ravn, H. P.: The spread of *Ips typographus* (L.) (Coleoptera, Scolytidae) attacks following heavy windthrow in Denmark, analysed using GIS, For. Ecol. Manag., 148, 31–39, https://doi.org/10.1016/S0378-

1197 1127(00)00477-1, 2001.

1198 Yao, Y., Joetzjer, E., Ciais, P., Viovy, N., Cresto Aleina, F., Chave, J., Sack, L., Bartlett, M., Meir, P., Fisher, R.,

1199 and Luyssaert, S.: Forest fluxes and mortality response to drought: model description (ORCHIDEE-CAN-NHA

1200 r7236) and evaluation at the Caxiuanã drought experiment, Geosci. Model Dev., 15, 7809–7833,

1201 https://doi.org/10.5194/gmd-15-7809-2022, 2022.

1202 Yi-Ying, C., Gardiner, B., Pasztor, F., Blennow, K., Ryder, J., Valade, A., Naudts, K., Otto, J., McGrath, M. J., and

1203 Planque, C.: Simulating damage for wind storms in the land surface model ORCHIDEE-CAN (revision 4262),

1204 Geosci. Model Dev., 11, 771, 2018.

1205 Yue, C., Ciais, P., Cadule, P., Thonicke, K., Archibald, S., Poulter, B., Hao, W. M., Hantson, S., Mouillot, F.,

1206 Friedlingstein, P., Maignan, F., and Viovy, N.: Modelling the role of fires in the terrestrial carbon balance by

1207 incorporating SPITFIRE into the global vegetation model ORCHIDEE – Part 1: simulating historical global burned

1208 area and fire regimes, Geosci. Model Dev., 7, 2747–2767, https://doi.org/10.5194/gmd-7-2747-2014, 2014.

1209 Zaehle, S. and Dalmonech, D.: Carbon–nitrogen interactions on land at global scales: current understanding in

1210 modelling climate biosphere feedbacks, Curr. Opin. Environ. Sustain., 3, 311–320,

1211 https://doi.org/10.1016/j.cosust.2011.08.008, 2011.

1212 Zaehle, S. and Friend, A. D.: Carbon and nitrogen cycle dynamics in the O-CN land surface model: 1. Model

1213 description, site-scale evaluation, and sensitivity to parameter estimates, Glob. Biogeochem. Cycles, 24,

1214 https://doi.org/10.1029/2009GB003521, 2010.

1215 Zhang, Q.-H. and Schlyter, F.: Olfactory recognition and behavioural avoidance of angiosperm nonhost volatiles by

1216 conifer-inhabiting bark beetles, Agric. For. Entomol., 6, 1–20, https://doi.org/10.1111/j.1461-9555.2004.00202.x,

1217 2004.

1218 Zscheischler, J., Westra, S., van den Hurk, B. J. J. M., Seneviratne, S. I., Ward, P. J., Pitman, A., AghaKouchak, A.,

1219 Bresch, D. N., Leonard, M., Wahl, T., and Zhang, X.: Future climate risk from compound events, Nat. Clim.

1220 Change, 8, 469–477, https://doi.org/10.1038/s41558-018-0156-3, 2018.

1221